ELSEVIER

INSTITUT PASTEUR

Microbes and Infection 13 (2011) 160–166

www.elsevier.com/locate/micinf

Original article

Effective recognition of HIV-1-infected cells by HIV-1 integrase-specific HLA-B*4002-restricted T cells

Tamayo Watanabe [a,b,1], Hayato Murakoshi [a,1], Hiroyuki Gatanaga [a,b], Madoka Koyanagi [a], Shinichi Oka [a,b,**], Masafumi Takiguchi [a,*]

[a] *Center for AIDS Research, Kumamoto University, 2-2-1 Honjo, Kumamoto 860-0811, Japan*
[b] *AIDS Clinical Center, National Center for Global Health and Medicine, 1-21-1 Toyama, Shinjuku-ku, Tokyo 162-8655, Japan*

Received 1 September 2010; accepted 13 October 2010
Available online 4 November 2010

Abstract

HLA-B*4002 is one of the common HLA-B alleles in the world. All 7 reported HLA-B*4002-restricted HIV epitopes are derived from Gag, Nef, and Vpr. In the present study we sought to identify novel HLA-B*4002-restricted HIV epitopes by using overlapping 11-mer peptides of HIV-1 Nef, Gag, and Pol, and found that 6 of these 11-mer Pol peptides included HLA-B*4002-restricted epitopes. Analysis using truncated peptides of these 6 peptides defined 4 optimal Pol (integrase) epitopes. All epitopes previously reported had Glu at position 2 (P2), suggesting that Glu at P2 is the anchor residue for HLA-B*4002; whereas only 2 of the integrase epitopes that we here identified had Glu at P2. CTL clones specific for the 2 epitopes effectively recognized HIV-1-infected cells whereas those for other 2 epitopes only weakly recognized them. The antigen sensitivity of the former clones for the epitope peptide was much higher than that of the latter clones, suggesting 2 possibilities: 1) the former T cells have high-affinity TCRs and/or 2) the epitope peptides recognized by the former T cells are highly presented by HLA-B*4002 in HIV-1-infected cells. These integrase-specific T cells with high antigen sensitivity may contribute to the suppression of HIV-1 replication in HIV-1-infected HLA-B*4002^{+} individuals.

Keywords: HIV-1; Cytotoxic T lymphocytes; HLA-B*4002; Integrase

1. Introduction

Human immunodeficiency virus type 1 (HIV-1)-specific cytotoxic T lymphocytes (CTL) play an important role in HIV-1 infections [1–4]. Previous studies demonstrated that HIV-1-specific CTL can inhibit viral replication in vitro [5–7] and that depletion of CD8^{+} T cells by treatment with an anti-CD8 mAb results in failure of the clearance of the virus in rhesus macaques infected with chimeric simian/human immunodeficiency virus [8]. These studies suggest that the CD8^{+} CTLs contribute to viral clearance and disease progression in HIV-1-infected individuals. The study of CTL responses in an African cohort demonstrated that HLA-B-restricted T cell responses are associated with lower viral load than HLA-A-restricted or HLA-C-restricted ones [9], suggesting that HLA-B-restricted responses are important for the control of HIV-1. Therefore, the characterization of HIV-1 epitope-specific HLA-B-restricted CTLs is important for understanding the pathogenesis of HIV and developing an AIDS vaccine.

HLA-B*4001 and HLA-B*4002 are common HLA-B alleles in the world. These alleles are found in 10.8% and 16.6% of Japanese population, respectively, and the frequency of HLA-B*4002 is the third highest among HLA-B alleles [10]. Only residue 97 differs between these 2 alleles. So far 10 HLA-B*4001-restricted and 7 HLA-B*4002-restricted HIV epitopes have been reported in Caucasian cohorts [11–16]. These HLA-B*4002-restricted epitopes were derived from

* Corresponding author. Tel.: +81 96 373 6529; fax: +81 96 373 6532.
** Tel./fax: +81 3 5273 5193.
E-mail addresses: oka@acc.ncgm.go.jp (S. Oka), masafumi@kumamoto-u.ac.jp (M. Takiguchi).
[1] Equally contributed.

1286-4579/$ - see front matter © 2010 Institut Pasteur. Published by Elsevier Masson SAS. All rights reserved.
doi:10.1016/j.micinf.2010.10.006

Gag, Nef, and Vpr; whereas the HLA-B*4001-restricted ones came from Gag, Nef, Pol, and Env.

In the present study, we sought to identify HLA-B*4001-restricted and HLA-B*4002-restricted HIV-1 epitopes in chronically HIV-1-infected Japanese cohorts by using 11-mer overlapping peptides derived from Pol, Gag, and Nef. We focused on these 3 proteins in the present study because these major proteins, which provide many CTL epitopes, are considered as vaccine targets. In addition, $CD8^+$ T cell clones specific for these newly identified epitopes were generated and used to clarify their ability to recognize HIV-1-infected cells. In the present study, we found 4 novel integrase epitopes presented by HLA-B*4002 and further characterized the $CD8^+$ T cells specific for these epitopes. Two of these epitopes were considered as immunodominant epitopes, because the specific T cells effectively recognized HIV-1-infected cells.

2. Materials and methods

2.1. Samples of HIV-1-infected individuals

This study was approved by the National Center for Global Health and Medicine and the Kumamoto University Ethical Committee. Informed consent was obtained from all subjects according to the Declaration of Helsinki. Peripheral blood mononuclear cells (PBMCs) were separated from heparinized whole blood. The HLA type of the patients was determined by standard sequence-based genotyping.

2.2. Synthetic peptides

We previously designed and generated overlapping peptides consisting of 11-mer amino acids and spanning Gag, Pol, and Nef of HIV-1 clade B consensus sequences [17]. Each 11-mer peptide was overlapped by 9 amino acids. Truncated peptides of some 11-mer peptides were synthesized by utilizing an automated multiple peptide synthesizer and purified by high-performance liquid chromatography (HPLC). The purity was examined by HPLC and mass spectrometry. Peptides with more than 90% purity were used in the present study.

2.3. Cells

The EBV-transformed B-lymphoblastoid cell lines (B-LCL) were established by transforming B cells from PBMC of KI-400. C1R cells expressing HLA-A*0207 (C1R-A*0207) and those expressing HLA-B*4002 (C1R-B*4002) were generated by transfecting C1R cells with the HLA-A*0207 and HLA-B*4002 genes, respectively. C1R-A*3101 cells were previously generated [18]. 721.221-CD4 cells expressing HLA-B*4002 (.221-CD4-B*4002), HLA-Cw*0102 (.221-CD4-Cw*0102), and HLA-Cw*0304(.221-CD4-Cw*0304) were generated by transfecting 721.221-CD4 cells with the HLA-B*4002, HLA-Cw*0102, and HLA-Cw*0304 genes, respectively, and maintained in RPMI 1640 medium supplemented with 10% FCS and 2.0 mg/ml hygromycin B.

2.4. Intracellular cytokine production (ICC) assay

PBMCs from chronically HIV-1-infected patient KI-400 were stimulated with HIV-1-derived peptide (1 μM) in culture medium (RPMI 1640 medium supplemented with 10% FCS and 200 U/ml recombinant human IL-2). After 14 days in culture, the cells were assessed for IFN-γ production activity by using a FACSCalibur. Briefly, bulk cultures were stimulated with stimulator cells pulsed with HIV-1-derived peptide (1 μM) for 2 h at 37 °C. Brefeldin A (10 μg/ml) was then added, and the cultures were continued for an additional 4 h. Cells were collected and stained with phycoerythrin (PE)-labelled anti-CD8 monoclonal antibody (mAb; Dako Corporation, Glostrup, Denmark). After having been treated with 4% paraformaldehyde solution, the cells were made permeable by incubation in permeabilization buffer (0.1% saponin and 20% NCS in phosphate-buffered saline) at 4 °C for 10 min and then stained with fluorescein isothiocyanate (FITC)-labeled anti-IFN-γ mAb (PharMingen, San Diego, CA). After a thorough washing with the permeabilization buffer, the cells were analyzed by using the FACSCalibur. Similarly IFN-γ production of established CTL clones was analyzed by use of this assay.

2.5. Generation of CTL clones

Peptide-specific CTL clones were generated from established peptide-specific bulk CTLs by seeding 0.8 cells/well into U-bottomed 96-well microtiter plates (Nunc, Roskilde, Denmark) together with 200 μl of cloning mixture (RPMI 1640 medium containing 10% FCS, 200 U/ml human recombinant interleukin-2, 5×10^5 irradiated allogeneic PBMCs from a healthy donor, and 1×10^5 irradiated C1R-B*4002 cells pulsed with a 1 μM concentration of the appropriate HIV-1-derived peptides. Wells positive for growth after about 2 weeks were examined for CTL activity by performing the ICC assay. All CTL clones were cultured in RPMI 1640 containing 10% FCS and 200 U/ml recombinant human interleukin-2. CTL clones were stimulated biweekly with irradiated target cells pulsed with the corresponding peptides.

2.6. HIV-1 clones

NL-432, which is an infectious proviral clone of HIV-1, was previously reported [7,19].

2.7. HIV-1 infection of .221-CD4-B*4002 and .221-CD4 cells

.221-CD4-B*4002 and 721.221-CD4 cells were exposed to NL-432 for several days. These infected cells were used as stimulator cells for ICC assays when approximately 60% of cells had been infected, which was confirmed by intracellular staining for HIV-1 p24 antigen.

3. Results

3.1. Identification of 11-mer peptides recognized by HLA-B*4001-restricted and HLA-B*4002-restricted HIV-1-specific CD8$^+$ T cells

To identify novel HLA-B*4001-restricted CTL epitopes, we analyzed 5 HIV-seropositive HLA-B*4001$^+$ Japanese individuals by Elispot assays with cocktails of overlapping 11-mer peptides spanning Gag (p17^{Gag}, p24^{Gag}, p2p7p1p6^{Gag}), Pol (Protease, RT, integrase), and Nef. The overlapping 11-mer peptide cocktails that gave more than 200 spots per 10^6 cells were used to stimulate PBMC of each patient in order to identify the epitopes. After the PBMC had been cultured for 2 weeks, their IFN-γ production was analyzed by using the ICC assay. We found that 3 peptide cocktails induced IFN-γ production. Further analysis using 10 peptides in the peptide cocktails showed that three 11-mer peptides included HLA-B*4001-restricted epitopes but all of these peptides contained reported HLA-B*4001-restricted epitope sequences. Thus, we could not find any novel HLA-B*4001-restricted epitopes.

In order to identify CTL epitopes restricted by HLA-B*4002, we analyzed fresh CD8$^+$ T cells from patient KI-400 (A*0207/A*3101, B*4002/B*4601, Cw*0102/Cw*0304) by performing Elispot assays with the cocktails of the overlapping 11-mer peptides. More than 200 spots per 10^6 cells were observed with 7 out of 25 Gag cocktails, 11 out of 50 Pol cocktails, and 1 out of 10 Nef cocktails (data not shown). To find novel HLA-B*4002-restricted CTL epitopes, we focused on analyzing 5 peptide cocktails (Gag21-49, Pol781-809, Pol801-829, Pol901-929, and Pol921-949) that did not contain reported epitopes restricted by the 6 HLA-class I alleles this patient expressed. To determine which peptide in each cocktail induced the specific CD8$^+$ T cells, we stimulated PBMCs from KI-400 with these peptide cocktails and then cultured the cells for 2 weeks. The responsiveness of the cultured CD8$^+$ T cells toward ten 11-mer peptides in each peptide cocktail was measured by using the ICC assay. IFN-γ production was found in the bulk CD8$^+$ T cells stimulated with autologous B-LCLs pre-pulsed with 2 Gag (Gag31-41 and Gag33-43) and 6 Pol peptides (Pol799-809, Pol807-817, Pol909-919, Pol911-921, Pol919-929, and Pol921-931).

For determination of HLA restriction molecules of CD8$^+$ T cells specific for these 11-mer peptides, the responsiveness of the bulk CD8$^+$ T cells towards peptide-pulsed C1R cells expressing one of the HLA-A or -B alleles or .221 cells expressing one of the HLA-C alleles was measured by performing the ICC assay. HLA-B*4002-restricted responses were found in the bulk culture cells stimulated with the cells pre-pulsed with Pol799-809, Pol807-817, Pol909-919, Pol911-921, Pol919-929 or Pol921-931 (data not shown). These results indicate that these six 11-mer peptides included HLA-B*4002-restricted epitopes.

3.2. Identification of HLA-B*4002-restricted optimal epitope peptides

To determine the optimal epitopes for these 11-mer peptides, we stimulated bulk T cells with C1R-B*4002 cells pre-pulsed with truncated peptide of Pol799-809, Pol807-817, Pol909-919, Pol911-921, Pol919-929 or Pol921-931 at concentrations of 1000 nM and then measured the IFN-γ production of each bulk T cells was measured by conducting the ICC assay. Previous studies on HLA-B*4002-restricted epitopes suggested that Glu at position 2 is an anchor for HLA-B*4002 (11–16). Judging from the finding that Pol801-811 did not include HLA-B*4002-restricted epitopes, we speculated that 2E in Pol799-809 (IG11: IEAEVIPAETG) would be the anchor for HLA-B*4002 rather than 4E. We therefore generated 5 truncated peptides (IT10: IEAEVIPAET, IA8: IEAEVIPA, ET9: EAEVIPAET, AT8: AEVIPAET, and AG9: AEVIPAETG) of Pol799-809 and investigated whether CD8$^+$ T cells induced by Pol799-809 would recognize these peptides. The T cells recognized only IG11 and IT10 at 1000 nM (Fig. 1A), whereas they showed higher sensitivity to IT10 than to IG11 (Fig. 1B). These findings indicate that Pol799-808 (IT10) was the optimal epitope.

For Pol807-817 (EL11: ETGQETAYFLL), we generated 4 truncated peptides (TL10: TGQETAYFLL, GL9: GQETAYFLL, GL8: GQETAYFL, and QL8: QETAYFLL). CD8$^+$ T cells induced by the Pol807-817 peptide recognized EL11, TL10, GL9 and QL8, but not GL8 (Fig. 1A), indicating that L at position 11 was critical for the epitope. On the other hand, the T cells showed higher sensitivity to EL11 than to the other 3 peptides (Fig. 1C). These findings indicate that Pol807-817 (EL11) was the optimal epitope.

For Pol909-919 (YI11: YSAGERIVDII) and Pol911-921 (AT11: AGERIVDIIAT), we assumed 2 possibilities: 1) the two 11-mer peptides shared the same epitope, or 2) the two peptides included different epitopes. To clarify these possibilities, we analyzed Pol909-919 and Pol911-921 independently. For Pol909-919, we generated 5 truncated peptides (SI10: SAGERIVDII, SI9: SAGERIVDI, AI8: AGERIVDI, AI9: AGERIVDII, and GI8: GERIVDII). CD8$^+$ T cells induced by Pol909-919 peptide recognized YI11, SI10, AI9, and GI8, but not SI9 and AI8 (Fig. 1A), indicating that I at position 11 was critical for this epitope. On the other hand, they showed higher sensitivity to GI8 than to the other 3 peptides (Fig. 1D). These findings indicate that Pol909-919 (GI8) was the optimal epitope. Regarding Pol911-921 (AT11), we generated 4 truncated peptides (AI9: AGERIVDII, AI8: AGERIVDI, GI8: GERIVDII, and GA9: GERIVDIIA). CD8$^+$ T cells induced by Pol911-921 peptide recognized AT11, AI9, GI8 and GA9, but not AI8 (Fig. 1A), indicating I at position 11 to be critical for this epitope. They also showed higher sensitivity to GI8 than to the other 3 peptides (Fig. 1E), indicating that GI8 (Pol912-919) was the optimal epitope. Thus, these results confirmed that Pol909-919 and Pol911-921 included the same epitope.

For Pol919-929 (IQ11: IATDIQTKELQ) and Pol921-931 (TQ11: TDIQTKELQKQ), we assumed that these two 11-mer peptides shared the same epitope. Therefore, we analyzed Pol919-929 and Pol921-931 independently. Regarding Pol919-929 (IQ11: IATDIQTKELQ) we speculated that 10L would be the C-terminus of the epitope because no hydrophilic residue is found in the C-terminus of HLA class I-binding peptides.

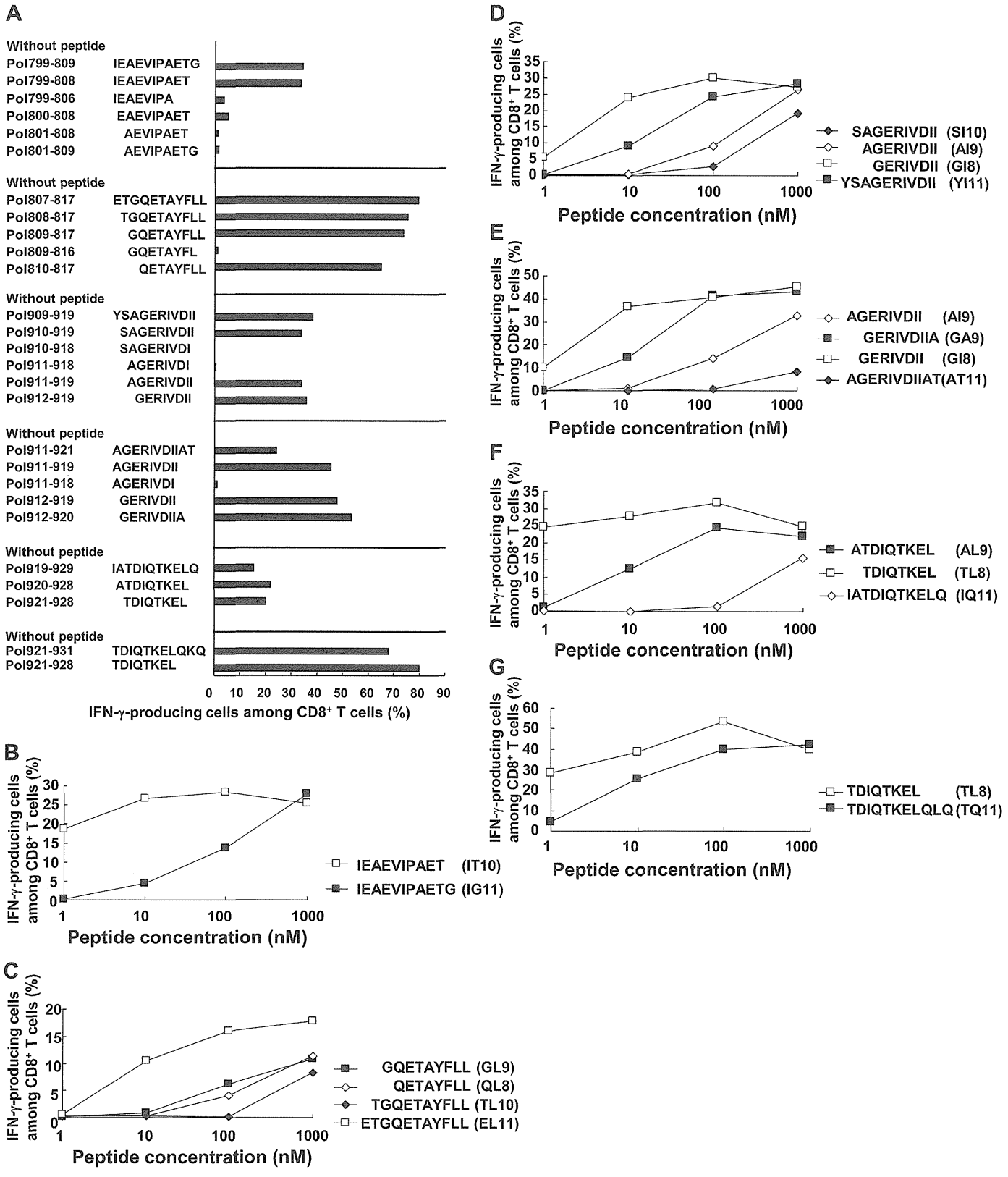

Fig. 1. Identification of HLA-B*4002-restricted HIV-1 CTL epitopes. A. For determination of the optimal epitopes of Pol799-809, Pol807-817, Pol909-919, Pol911-921, Pol919-929 and Pol921-931, the recognition of the bulk T cells for the truncated peptides was examined by using C1R-B*4002 cells pre-pulsed with each truncated peptide at a concentration of 1000 nM. The responsiveness of the bulk $CD8^+$ T cells toward each truncated peptide was measured by using the ICC assay. The percentages of IFN-γ-producing cells among the $CD8^+$ T cells are shown in the figure. B–G. Optimal epitopes were not determined at concentrations of 1000 nM for Pol799-809 (B), Pol807-817 (C), Pol909-919 (D), Pol911-921 (E), Pol919-929 (F) or Pol921-931 (G). The responsiveness of the bulk $CD8^+$ T cells was examined for C1R-B*4002 cells pre-pulsed with each truncated peptide at concentrations from 1 to 1000 nM. The responsiveness of the bulk $CD8^+$ T cells toward each truncated peptide was measured by performing the ICC assay. The percentages of IFN-γ-producing cells among $CD8^+$ T cells are shown in the figure.

Therefore, we generated 2 truncated peptides (AL9: ATDIQTKEL and TL8: TDIQTKEL). Bulk $CD8^+$ T cells induced by Pol919-929 peptide recognized all 3 peptides (Fig. 1A) and showed higher sensitivity to TL8 than to the other 2 peptides (Fig. 1F), indicating that Pol921-928 (TL8) was the optimal epitope. Similarly we speculated TL8 to be optimal epitope for Pol921-931 (TQ11: TDIQTKELQKQ), because no hydrophilic residue is found in the C-terminus of HLA-class I-restricted epitopes. Although bulk $CD8^+$ T cells induced by Pol921-931 peptide recognized both TQ11 and TL8 peptides (Fig. 1A), they showed higher sensitivity to TL8 than to TQ11 (Fig. 1F). These findings indicate that Pol919-929 and Pol921-931 11-mer peptides included the same epitope, Pol921-928(TL8).

Thus, we identified 4 HLA-B*4002-restricted optimal peptides. Interestingly, these 4 Pol epitopes were all derived from integrase.

*3.3. Generation and antigen sensitivity of HLA-B*4002-restricted Pol-specific CTL clones*

To analyze the $CD8^+$ T cells specific for these 4 integrase epitopes, IT10 (Pol799-808), EL11 (Pol807-817), GI8 (Pol912-919), and TL8 (Pol921-928), we established the specific $CD8^+$ T cell clones and analyzed them for their antigen sensitivity by using the ICC assays. The result was shown in Fig. 2. The T cell clones and their EC_{50} values were as follows: Pol799-808-specific T cells (27.7), Pol807-817-specific T cells (191.7), Pol912-919-specific T cells (443.1), and Pol921-928-specific T cells (7.6). These results indicate that Pol799-808-specific and Pol921-928-specific $CD8^+$ T cell clones had higher antigen sensitivity than Pol807-817-specific and Pol912-919-specific ones.

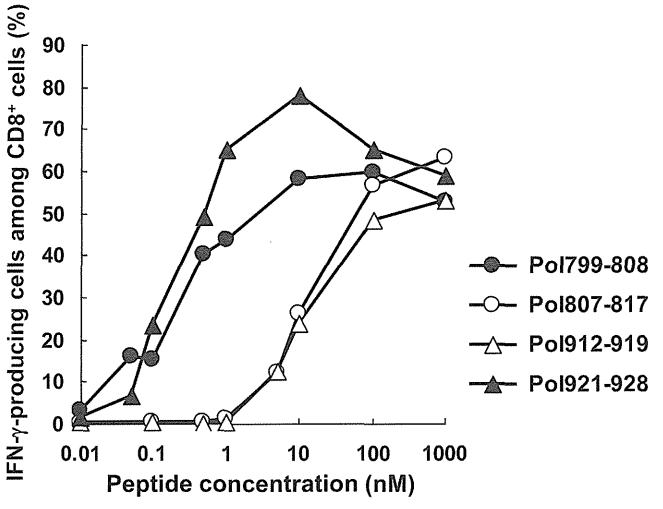

Fig. 2. Antigen Sensitivity of 4 HIV-1 integrase-specific $CD8^+$ T cells. Antigen sensitivity of 4 HIV-1 integrase-specific $CD8^+$ T cells was examined by using the ICC assay. The responsiveness of these CTL clones was examined for C1R-B*4002 cells pre-pulsed with each truncated peptide at concentrations from 0.01 to 1000 nM.

3.4. Recognition of HIV-1-infected cells by specific T cells

To clarify whether Pol799-808, Pol807-817, Pol912-919, and Pol921-928 were naturally occurring peptides and whether CTLs specific for these epitopes had the ability to recognize HIV-1-infected cells, we investigated the response of these peptide-specific $CD8^+$ T cell clones toward HIV-1 (NL-432)-infected .221-CD4 cell lines expressing HLA-B*4002. NL-432 includes wild-type sequences of these 4 epitopes. .221-CD4 cell lines and those expressing HLA-B*4002 were infected with NL-432, and then cultured for 4 days. The responses of the T cell clones toward these infected cells were measured by using the ICC assay. The percentage of the HIV-1-infected cells was determined by staining intracellular HIV-1 p24 (Fig. 3A). The Pol799-808-specific, Pol807-817-specific, Pol912-919-specific, and Pol921-928-specific CTL clones responded to .221-CD4-B*4002 cells infected with HIV-1 but not to uninfected .221-CD4-B*4002 cells or to HLA-B*4002-negative .221-CD4 cells infected with HIV-1. These results indicate that Pol799-808, Pol807-817, and Pol921-928 peptides were naturally processed and presented by HLA-B*4002 and that the T cells specific for these epitopes could recognize HIV-1-infected cells (Fig. 3B). On the other hand, the responses of Pol807-817-specific and Pol912-919-specific CTL clones was much weaker than those of the other CTL clones (Fig. 3B), indicating that the former CTLs only weakly recognized HIV-1-infected cells.

4. Discussion

There is only 1 amino acid substitution, at residue 97, on the peptide binding floor between HLA-B*4001 and HLA-B*4002. A previous study on the peptide motif of HLA-B*4001 showed that HLA-B*4001-binding peptide anchors are Glu at P2 (2E) and Leu at the C-terminus [20]. Indeed, 7 of 8 reported HLA-B*4001-restricted HIV-1-specific T cell epitopes have 2E and Leu at their C-terminus [11–13]. Although no HLA-B*4002-binding peptide motif had not yet been identified, we speculated that this motif would be similar to the HLA-B*4001-binding one. Indeed, all 7 HLA-B*4002-restricted epitopes previously reported have 2E (Table 1). However, 2 of the 4 epitopes identified in the present study did not have the 2E anchor. In addition, only 5 of 11 HLA-B*4002-restricted epitopes had Leu at their C-terminus. These findings suggest that the substitution from Ser to Arg at residue 97 may partially affect the structure of the F and B pockets. Pol807-817 (ETGQETAYFLL) does not have the 2E anchor. QL8 (QETAYFLL) is speculated to be an HLA-B*4002-restricted epitope because this peptide has 2E. However, the antigen sensitivity of the T cells specific for QL8 is much weaker than that for EL11. This result excludes the possibility that QL8 is the epitope peptide. Thr at position 2 of Pol807-817 may bind to the residues facing the B-pocket by hydrogen-bonding. Nine of the 11 HLA-B*4002-restricted epitopes have 2E, suggesting that the 2E is still anchor residue for HLA-B*4002.

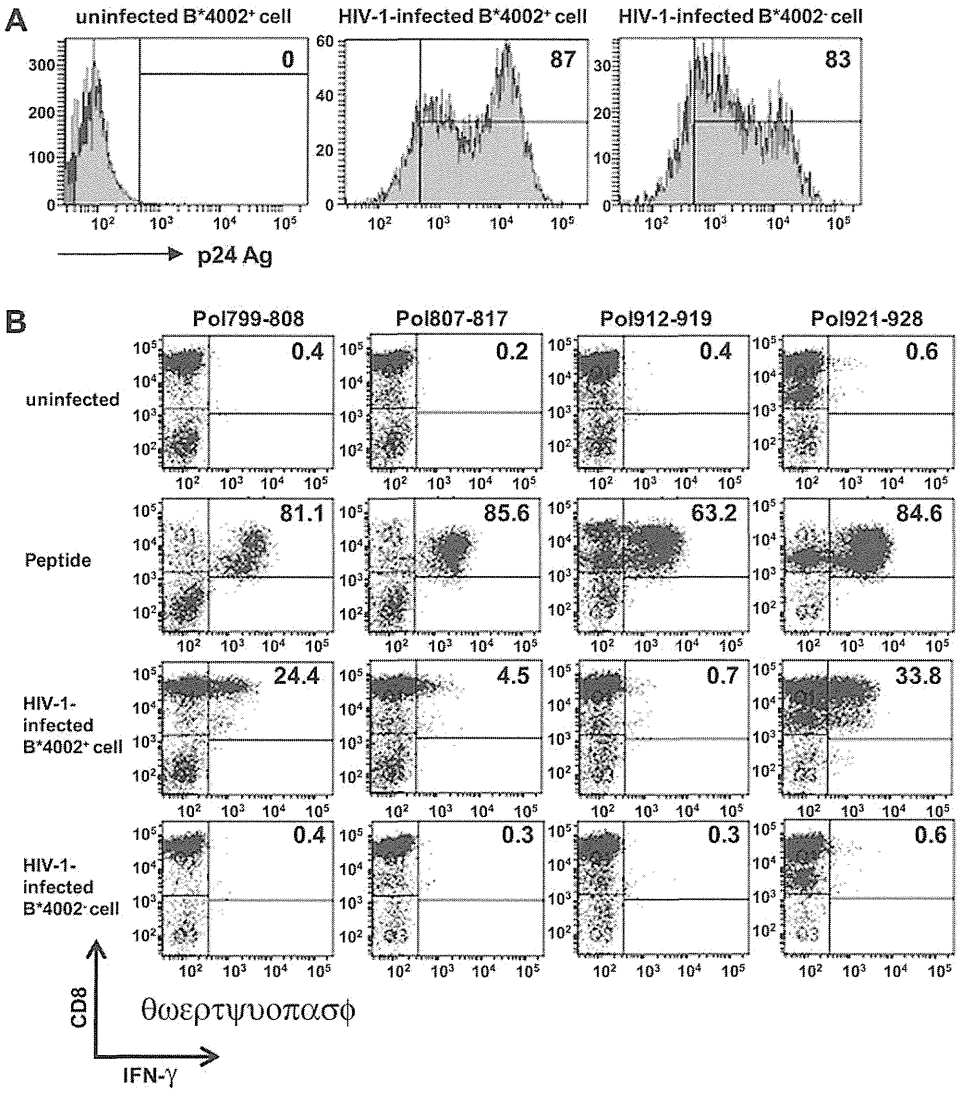

Fig. 3. Ability of 4 HIV-1 integrase-specific $CD8^+$ T cells to recognize HIV-1-infected cells. A. The .221-CD4 and $B*4002^+$.221-CD4 cell lines were infected with HIV-1 (NL-432) and cultured for 4 days. The frequency of HIV-1-infected cells was detected by using staining of intracellular p24 with anti-p24 mAb. The percentage of HIV-1-infected cells is shown in each figure. B. Recognition of HIV-1-infected cells by the Pol799-808-, Pol807-817-, Pol912-919- or Pol921-928-specific $CD8^+$ T cell clones. The activities of these peptide-specific $CD8^+$ T cell clones to recognize $B*4002^+$.221-CD4 cell lines infected with HIV-1 or those pre-pulsed with the corresponding peptide (1000 nM) were measured by use of the ICC assay. The percentages of IFN-γ-producing cells among $CD8^+$ T cells are shown in each figure.

Although the 7 HLA-B*4002-restricted epitopes previously reported do not include Pol-derived ones, we identified novel 4 HLA-B*4002-retricted Pol-specific T cell epitopes in the present study. Interestingly, all of these Pol epitopes were derived from integrase. Though 29 integrase epitopes were reported as 20 different HLA class I-restricted epitopes (Los Alamos HIV Molecular Immunology Data), integrase epitopes were not found among HLA-B*4001-restricted Pol epitopes. Regarding the integrase epitopes, HLA-B*4201 and HLA-B*1503 present 3 different epitopes, whereas the other 18 alleles present 1 or 2 epitopes. Thus, HLA-B*4002 is so far the only HLA-class I allele that can present more than 3 integrase epitopes.

Pol799-808-specific and Pol921-928-specific T cells strongly recognized HIV-1-infected cells, whereas Pol807-817-specific and Pol912-919-specific ones weakly recognized these cells. Antigen sensitivity of the former T cells was much higher than that of the latter ones. Thus, the ability to recognize HIV-1-infected cells was associated with the antigen sensitivity. However, it is difficult to clarify why the 2 T cells weakly recognize HIV-1-infected cells because we did not measure the bindings of these epitope peptides to HLA-B*4002 molecules and of the specific tetramers to the specific T cells. We can suggest 2 possibilities from the data shown in Fig. 2 and Fig. 3: 1) The former T cells may have higher affinity TCR and/or 2) these former epitope peptides are more highly presented than the latter by HLA-B*4002 in HIV-1-infected cells. Since Pol799-808-specific and Pol921-928-specific T cells strongly recognized HIV-1-infected cells, we proposed that they would effectively recognize and kill HIV-1-infected cells *in vivo*.

HLA-B*4001 and HLA-B*4002 are found in 10.8% and 16.6% of the Japanese population, respectively. Since both

Table 1
A list of HLA-B*4002-restricted epitopes identified previously and in this study.

Sequence	Protein	Reference
GELDRWEKI	Gag (p17)	*15
KETINEEAA	Gag (p24)	*15
AEWDRVHPV	Gag (p24)	*15
AEAMSQVTNS	Gag (p2p7p1p6)	*16
TERQANFL	Gag (p2p7p1p6)	*15
REPHNEWTL	Vpr	*14
KEKGGLEGL	Nef	*15
IEAEVIPAET	Pol (Integrase)	This study (Pol799-808)
ETGQETAYFLL	Pol (Integrase)	This study (Pol807-817)
GERIVDII	Pol (Integrase)	This study (Pol912-919)
TDIQTKEL	Pol (Integrase)	This study (Pol921-928)

HLA-class I alleles are detected in approximately 25% of Japanese individuals, T cell epitopes presented by these alleles are useful for studies on HIV-1 immunopathogenesis and the development of AIDS vaccines.

Acknowledgments

The authors thank Sachiko Sakai for secretarial assistance. This research was supported by the Program of Founding Research Centers for Emerging and Reemerging Infectious Diseases and by the Global COE program "Global Education and Research Center Aiming at the control of AIDS" supported by the Ministry of Education, Science, Sports and Culture, Japan; by a grant-in-aid (No. 20390134) for scientific research from the Ministry of Health, Japan; and by a grant-in-aid (No. 18390141) for scientific research from the Ministry of Education, Science, Sports and Culture, Japan.

References

[1] R.A. Koup, J.T. Safrit, Y. Cao, C.A. Andrews, G. McLeod, W. Borkowsky, C. Farthing, D.D. Ho, Temporal association of cellular immune responses with the initial control of viremia in primary human immunodeficiency virus type 1 syndrome, J. Virol. 68 (1994) 4650–4655.

[2] G. Pantaleo, J.F. Demarest, H. Soudeyns, C. Graziosi, F. Denis, J.W. Adelsberger, P. Borrow, M.S. Saag, G.M. Shaw, P.S. Sekaly, A.S. Fauci, Major expansion of $CD8^+$ T cells with a predominant Vβ usage during the primary immune response to HIV, Nature 370 (1994) 463–467.

[3] P.A. Moss, S.L. Rowland-Jones, P.M. Frodsham, S. McAdam, P. Giangrande, A.J. McMichael, J.I. Bell, Persistent high frequency of human immunodeficiency virus-specific cytotoxic T cells in peripheral blood of infected donors, Proc. Natl. Acad. Sci. U S A 92 (1995) 5773–5777.

[4] S. Rowland-Jones, J. Sutton, K. Ariyoshi, T. Dong, F. Gotch, S. McAdam, D. Whitby, S. Sabally, A. Gallimore, T. Corrah, M. Takiguchi, T. Schultz, A. McMichael, H. Whittle, HIV-1 specific cytotoxic T cells in HIV-exposed but uninfected Gambian women, Nat. Med. 1 (1995) 59–64.

[5] C.M. Walker, D.J. Moody, D.P. Stites, J.A. Levy, $CD8^+$ lymphocytes can control HIV infection in vitro by suppressing virus replication, Science 234 (1986) 1563–1566.

[6] O.O. Yang, B.D. Walker, $CD8^+$ cells in human immunodeficiency virus type I pathogenesis: cytolytic and noncytolytic inhibition of viral replication, Adv. Immunol. 66 (1997) 273–311.

[7] H. Tomiyama, H. Akari, A. Adachi, M. Takiguchi, Different effects of Nef-mediated HLA class I down-regulation on human immunodeficiency virus type 1-specific $CD8^+$ T-cell cytolytic activity and cytokine production, J. Virol. 76 (2002) 7535–7543.

[8] T. Matano, R. Shibata, C. Siemon, M. Connors, H.C. Lane, M.A. Martin, Administration of an anti-CD8 monoclonal antibody interferes with the clearance of chimeric simian/human immunodeficiency virus during primary infections of rhesus macaques, J. Virol. 72 (1998) 164–169.

[9] P. Kiepiela, A.J. Leslie, I. Honeyborne, D. Ramduth, C. Thobakgale, S. Chetty, P. Rathnavalu, C. Moore, K.J. Pfafferott, L. Hilton, P. Zimbwa, S. Moore, T. Allen, C. Brander, M.M. Addo, M. Altfeld, I. James, S. Mallal, M. Bunce, L.D. Barber, J. Szinger, C. Day, P. Klenerman, J. Mullins, B. Korber, H.M. Coovadia, B.D. Walker, P.J. Goulder, Dominant influence of HLA-B in mediating the potential co-evolution of HIV and HLA, Nature 432 (2004) 769–775.

[10] Y. Itoh, N. Mizuki, T. Shimada, F. Azuma, M. Itakura, K. Kashiwase, E. Kikkawa, J.K. Kulski, M. Satake, H. Inoko, High-throughput DNA typing of HLA-A, -B, -C, and -DRB1 loci by a PCR-SSOP-Luminex method in the Japanese population, Immunogenetics 57 (2005) 717–729.

[11] M.A. Altfeld, A. Trocha, R.L. Eldridge, E.S. Rosenberg, M.N. Phillips, M.M. Addo, R.P. Sekaly, S.A. Kalams, S.A. Burchett, K. McIntosh, B.D. Walker, P.J. Goulder, Identification of dominant optimal HLA-B60- and HLA-B61-restricted cytotoxic T-lymphocyte (CTL) epitopes: rapid characterization of CTL responses by enzyme-linked immunospot assay, J. Virol. 74 (2000) 8541–8549.

[12] X.G. Yu, H. Shang, M.M. Addo, R.L. Eldridge, M.N. Phillips, M.E. Feeney, D. Strick, C. Brander, P.J. Goulder, E.S. Rosenberg, B.D. Walker, M. Altfeld, Important contribution of p15 Gag-specific responses to the total Gag-specific CTL responses, AIDS 16 (2002) 321–328.

[13] R. Draenert, T.M. Allen, Y. Liu, T. Wrin, C. Chappey, C.L. Verrill, G. Sirera, R.L. Eldridge, M.P. Lahaie, L. Ruiz, B. Clotet, C.J. Petropoulos, B.D. Walker, J. Martinez-Picado, Constraints on HIV-1 evolution and immunodominance revealed in monozygotic adult twins infected with the same virus, J. Exp. Med. 203 (2006) 529–539.

[14] M. Altfeld, M.M. Addo, R.L. Eldridge, X.G. Yu, S. Thomas, A. Khatri, D. Strick, M.N. Phillips, G.B. Cohen, S.A. Islam, S.A. Kalams, C. Brander, P.J. Goulder, E.S. Rosenberg, B.D. Walker, Vpr is preferentially targeted by CTL during HIV-1 infection, J. Immunol. 167 (2001) 2743–2752.

[15] S. Sabbaj, A. Bansal, G.D. Ritter, C. Perkins, B.H. Edwards, E. Gough, J. Tang, J.J. Szinger, B. Korber, C.M. Wilson, R.A. Kaslow, M.J. Mulligan, P.A. Goepfert, Cross-reactive CD8+ T cell epitopes identified in US adolescent minorities, J. Acquir. Immune. Defic. Syndr. 33 (2003) 426–438.

[16] T. Bhattacharya, M. Daniels, D. Heckerman, B. Foley, N. Frahm, C. Kadie, J. Carlson, K. Yusim, B. McMahon, B. Gaschen, S. Mallal, J.I. Mullins, D.C. Nickle, J. Herbeck, C. Rousseau, G.H. Learn, T. Miura, C. Brander, B. Walker, B. Korber, Founder effects in the assessment of HIV polymorphisms and HLA allele associations, Science 315 (2007) 1583–1586.

[17] H. Murakoshi, M. Kitano, T. Akahoshi, Y. Kawashima, S. Dohki, S. Oka, M. Takiguchi, Identification and characterization of 2 HIV-1 Gag immunodominant epitopes restricted by Asian HLA allele HLA-B*4801, Hum. Immunol. 70 (2009) 170–174.

[18] M.A. Borghan, S. Oka, M. Takiguchi, Identification of HLA-A*3101-restricted cytotoxic T-lymphocyte response to human immunodeficiency virus type 1 (HIV-1) in patients with chronic HIV-1 infection, Tissue Antigens 66 (2005) 305–313.

[19] H. Akari, S. Arold, T. Fukumori, T. Okazaki, K. Strebel, A. Adachi, Nef-induced major histocompatibility complex class I down-regulation is functionally dissociated from its virion incorporation, enhancement of viral infectivity, and CD4 down-regulation, J. Virol. 74 (2000) 2907–2912.

[20] K. Falk, O. Rotzschke, M. Takiguchi, V. Gnau, S. Stevanovic, G. Jung, H.G. Rammensee, Peptide motifs of HLA-B58, B60, B61, and B62 molecules, Immunogenetics 41 (1995) 165–168.

K70Q Adds High-Level Tenofovir Resistance to "Q151M Complex" HIV Reverse Transcriptase through the Enhanced Discrimination Mechanism

Atsuko Hachiya[1,2], Eiichi N. Kodama[3]*, Matthew M. Schuckmann[1], Karen A. Kirby[1], Eleftherios Michailidis[1], Yasuko Sakagami[4], Shinichi Oka[2], Kamalendra Singh[1], Stefan G. Sarafianos[1]*

1 Department of Molecular Microbiology and Immunology, University of Missouri School of Medicine, Columbia, Missouri, United States of America, **2** AIDS Clinical Center, National Center for Global Health and Medicine, Tokyo, Japan, **3** Division of Emerging Infectious Diseases, Tohoku University School of Medicine, Sendai, Japan, **4** Institute for Virus Research, Kyoto University, Kyoto, Japan

Abstract

HIV-1 carrying the "Q151M complex" reverse transcriptase (RT) mutations (A62V/V75I/F77L/F116Y/Q151M, or Q151Mc) is resistant to many FDA-approved nucleoside RT inhibitors (NRTIs), but has been considered susceptible to tenofovir disoproxil fumarate (TFV-DF or TDF). We have isolated from a TFV-DF-treated HIV patient a Q151Mc-containing clinical isolate with high phenotypic resistance to TFV-DF. Analysis of the genotypic and phenotypic testing over the course of this patient's therapy lead us to hypothesize that TFV-DF resistance emerged upon appearance of the previously unreported K70Q mutation in the Q151Mc background. Virological analysis showed that HIV with only K70Q was not significantly resistant to TFV-DF. However, addition of K70Q to the Q151Mc background significantly enhanced resistance to several approved NRTIs, and also resulted in high-level (10-fold) resistance to TFV-DF. Biochemical experiments established that the increased resistance to tenofovir is not the result of enhanced excision, as K70Q/Q151Mc RT exhibited diminished, rather than enhanced ATP-based primer unblocking activity. Pre-steady state kinetic analysis of the recombinant enzymes demonstrated that addition of the K70Q mutation selectively decreases the binding of tenofovir-diphosphate (TFV-DP), resulting in reduced incorporation of TFV into the nascent DNA chain. Molecular dynamics simulations suggest that changes in the hydrogen bonding pattern in the polymerase active site of K70Q/Q151Mc RT may contribute to the observed changes in binding and incorporation of TFV-DP. The novel pattern of TFV-resistance may help adjust therapeutic strategies for NRTI-experienced patients with multi-drug resistant (MDR) mutations.

Citation: Hachiya A, Kodama EN, Schuckmann MM, Kirby KA, Michailidis E, et al. (2011) K70Q Adds High-Level Tenofovir Resistance to "Q151M Complex" HIV Reverse Transcriptase through the Enhanced Discrimination Mechanism. PLoS ONE 6(1): e16242. doi:10.1371/journal.pone.0016242

Editor: Zandrea Ambrose, University of Pittsburgh, United States of America

Received September 15, 2010; **Accepted** December 8, 2010; **Published** January 13, 2011

Funding: This work was supported by a grant for the promotion of AIDS Research from the Ministry of Health, Labor and Welfare (AH and EK, http://www.mhlw.go.jp/english/index.html), by grants from the Korea Food & Drug Administration and the Ministry of Knowledge and Economy, Bilateral International Collaborative R&D Program, Republic of Korea (SGS) and by National Institutes of Health (NIH, http://nih.gov/) research grants AI094715, AI076119, AI079801, and AI074389 to SGS. The funders had no role in study design, data collection and analysis, decision to publish, or preparation of the manuscript.

Competing Interests: The authors have declared that no competing interests exist.

* E-mail: sarafianoss@missouri.edu (SGS); kodama515@m.tains.tohoku.ac.jp (ENK)

Introduction

Nucleos(t)ide reverse transcriptase inhibitors (NRTIs) are used in combination with other classes of drugs for the treatment of patients infected with human immunodeficiency virus type-1 (HIV-1). This approach is known as highly active anti-retroviral therapy (HAART) and has been remarkably successful in reducing the viral loads and increasing the number of CD4+ cells in patients' plasma. However, prolonged therapies inevitably result in resistance to all of the available drugs. Several mutations in the reverse transcriptase (RT) are known to cause resistance to NRTIs through two basic mechanisms:

1) The excision mechanism, which is based on an enhanced capacity of RT to use adenosine triphosphate (ATP) as a nucleophile for the removal of the chain-terminating nucleotide from the DNA terminus. The excision reaction products are a 5′, 5′-dinucleoside tetraphosphate and an unblocked primer with a free 3′-OH, allowing DNA synthesis to resume [1,2,3]. Increased excision of NRTIs is imparted by Excision Enhancement Mutations, typically M41L, D67N, K70R, T215Y/F, L210W, and K219E/Q (also known as Thymidine Associated Mutations, or TAMs). Other mutations have also been reported to enhance excision, including insertions or deletions at the tip of the β3- β4 loop of the fingers subdomain in the background of other excision enhancement mutations [4,5,6,7,8,9,10,11].

2) The other mechanism of NRTI resistance is the exclusion mechanism, which is caused when NRTI-resistance mutations in RT enhance discrimination and reduce incorporation of the NRTI-triphosphate (NRTI-TP). This mechanism is exemplified by the resistance of the M184V RT mutant to lamivudine (3TC) and emtricitabine (FTC) due to steric clash between the β-branched Val or Ile at position 184 and the oxathiolane ring of the inhibitors [12,13]. Another example of the exclusion mechanism is the multi-drug resistant (MDR) HIV-1 RT known as Q151M complex (Q151Mc). This RT contains the Q151M mutation together with a cluster of four

additional mutations (A62V/V75I/F77L/F116Y) [14,15]. Q151M by itself causes intermediate- to high-level resistance to zidovudine (AZT), didanosine (ddI), zalcitabine (ddC), stavudine (d4T), and low level resistance to abacavir (ABC) [15,16,17] without reducing viral fitness [18,19]. Addition of the four associated mutations increases replication capacity of RT and results in high-level resistance to AZT, ddI, ddC, and d4T, 5-fold resistance to ABC and low-level resistance to lamivudine (3TC) and emtricitabine (FTC) [17,18,19,20,21]. Miller *et al.* and Smith *et al.* reported a 1.8-fold and 3.6-fold increase in resistance to tenofovir (TFV), respectively [22,23].

Biochemical studies on the mechanism of Q151Mc resistance to multiple NRTIs have revealed that the mutations of this complex decrease the maximum rate of NRTI-TP incorporation without significantly affecting the incorporation of the natural nucleotides [21,24,25]. Structurally, the Q151 residue interacts with the 3′-OH of a normal deoxynucleoside triphosphate (dNTP) substrate [26]. It appears that the Q151Mc mutations cause resistance to multiple NRTIs by affecting the hydrogen bond network involving protein side chains in the vicinity of the dNTP-binding site and the NRTI triphosphate lacking a 3′-OH [25,26,27]. The Q151Mc set of mutations was also reported to decrease pyrophosphate PPi- and ATP-mediated excision [25].

K65R is another mutation near the polymerase active site that confers NRTI resistance through the exclusion mechanism. Specifically, K65R RT has reduced susceptibility to the acyclic nucleotide analog, TFV and other NRTIs, including ddI, ddC, ABC, FTC and 3TC [28,29,30,31]. Biochemical studies with K65R RT have demonstrated that this enzyme decreases the incorporation rate of these NRTIs [32,33,34]. The crystal structure of K65R RT in complex with DNA and TFV diphosphate (TFV-DP) revealed that R65 forms a molecular platform with the conserved residue R72, and the platform enhances the ability of K65R RT to discriminate NRTIs from dNTPs [35]. HIV carrying the Q151Mc mutations has been reported to be susceptible to TFV disoproxil fumarate (TFV-DF), the oral prodrug of TFV that enhances its oral bioavailability and anti-HIV activity [22,36]. While the K65R mutation appeared in several patients treated for more than 18 months with TFV-DF, no patient developed multi-NRTI resistance through appearance of Q151Mc [37].

Here we report the identification of unique HIV clinical isolates that have acquired the K70Q mutation in the background of Q151Mc during TFV-DF-containing therapy. We have used a combination of virological, biochemical, and molecular modeling methods to derive the mechanism by which this mutation confers resistance to TFV.

Materials and Methods

Clinical samples

HIV was isolated from fresh plasma immediately after collection of clinical samples from study participants at the outpatient clinic of the AIDS Clinical Center (ACC), International Medical Center of Japan. The Institutional Review Board approved this study (IMCJ-H13-80) and a written consent was obtained from all participants.

Construction of recombinant clones of HIV-1

Recombinant infectious clones of HIV-1 carrying various mutations were prepared using standard site-directed mutagenesis protocols as described previously [38]. The NL4-3-based molecular clone was constructed by replacing the *pol*-coding region with the HIV-1 BH10 strain. Restriction enzyme sites *Xma I* and *Nhe I* were introduced by silent mutations into the molecular clone at positions corresponding to HIV-1 RT codons 15 and 267, respectively [39]. Each molecular clone was transfected into COS-7 cells. Cells were grown for 48 h, and culture supernatants were harvested and stored at −80°C until use.

Single-cycle drug susceptibility assay

Susceptibilities to various RT inhibitors were determined using the MAGIC-5 cells which are HeLa cells stably transfected with a β-galactosidase gene under the control of an HIV long terminal repeat promoter, and with vectors that express the CD4 receptor and the CCR5 co-receptor under the control of the CMV promoter as described previously [40]. Briefly, MAGIC-5 cells were infected with diluted virus stock (100 blue forming units) in the presence of increasing concentrations of RT inhibitors, cultured for 48 h, fixed, and stained with X-Gal (5-bromo-4-chloro-3-indolyl-β-D-galacto-pyranoside). The stained cells were counted under a light microscope. Drug concentrations reducing the number of infected cells to 50% of the drug-free control (EC_{50}) were determined from dose response curves.

Enzymes

RT sequences coding for the p66 and p51 subunits of BH10 were cloned in the pRT dual vector, which is derived from pCDF-2 with LIC duet minimal adaptor (Novagen), using restriction sites *PpuMI* and *SacI* for the p51 subunit, and *SacII* and *AvrII* for the p66 subunit. RT was expressed in the *Escherichia coli* strain BL21 (Invitrogen) and purified by nickel affinity chromatography and MonoQ anion exchange chromatography [41]. RT concentrations were determined spectrophotometrically based on absorption at 260 nm using a calculated extinction coefficient (261,610 M^{-1} cm^{-1}). The active site concentration of the various RT preparations was calculated as described below.

Nucleic acid substrates

DNA oligomers were synthesized by Integrated DNA Technologies (Coralville, IA). An 18-nucleotide DNA primer fluorescently labeled with Cy3 at the 5′ end (P_{18}; 5′-Cy3 GTC CCT GTT CGG GCG CCA-3′) and a 100-nucleotide DNA template (T_{100}; 5′-TAG TGT GTG CCC GTC TGT TGT GTG ACT CTG GTA ACT AGA GAT CCC TCA GAC CCT TTT AGT CAG TGT GGA AAA TCT CTA GCA GTG GCG CCC GAA CAG GGA C-3′) were used in primer extension assays. An 18-nucleotide DNA primer 5′-labeled with Cy3 (P_{18}; 5′-Cy3 GTC ACT GTT CGA GCA CCA-3′) and a 31-nucleotide DNA template (T_{31}; 5′- CCA TAG CTA GCA TTG GTG CTC GAA CAG TGA C-3′) were used in the ATP rescue assay and pre-steady state kinetic experiments.

Active site titration and determination of the dissociation constant for DNA binding ($K_{D\text{-}DNA}$)

Determination of active site concentrations in the different preparations of WT and mutant RTs were performed using pre-steady state burst experiments. A fixed concentration of RT (80 nM, determined by absorbance measurements) was pre-incubated with increasing concentrations of DNA/DNA template/primer (T_{31}/P_{18}), followed by rapidly mixing with a reaction mixture containing $MgCl_2$ and dATP, at final concentrations of 5 mM and 50 μM, respectively. The reactions were quenched at various times (10 ms to 5 s) by adding EDTA to a final concentration of 50 mM. The amounts of product (P_{18}-dAMP) were quantitated and fit to the following burst equation:

$$P = A(1 - e^{-kobst}) + k_{ss}t \quad (1)$$

where A is the amplitude of the burst phase that represents the RT-DNA complex at the start of the reaction, k_{obs} is the observed burst rate constant for dNTP incorporation, k_{ss} is the steady state rate constant, and t is the reaction time. The rate constant of the linear phase (k_{cat}) can be estimated by dividing the slope of the linear phase by the enzyme concentration. The active site concentration and template/primer binding affinity ($K_{D\text{-}DNA}$) were determined by plotting the amplitude (A) against the concentration of template/primer. The data were fit using non-linear regression to a quadratic equation:

$$A = 0.5(K_D + [RT] + [DNA]) - \sqrt{0.25(K_D + [RT] + [DNA])^2 - ([RT][DNA])} \quad (2)$$

where K_D is the dissociation constant for the RT-DNA complex, and [RT] is the concentration of active polymerase molecules. Subsequent biochemical experiments were performed using corrected active site concentrations [42,43].

Primer extension assay

To examine the DNA polymerase activity of WT and mutant RTs and the inhibition of DNA synthesis by TFV, the primer extension assays were carried out on the T_{100}/P_{18} template/primer (P_{18} was 5′-Cy3 labeled) in the presence or absence of 3.5 mM ATP [41]. The enzyme (20 nM active sites) was incubated with 20 nM template/primer at 37°C in a buffer containing 50 mM Tris-HCl, pH 7.8 and 50 mM NaCl. The DNA synthesis was initiated by the addition of 1 μM dNTP and 10 mM $MgCl_2$. The primer extension assays were carried out in the presence or absence of varying concentrations of TFV-DP. The reactions were terminated after 15 min by adding equal volume of 100% formamide containing traces of bromophenol blue. The extension products were resolved on a 7 M urea-15% polyacrylamide gel, and visualized by phosphor-imaging (FLA 5100, Fujifilm, Tokyo). We followed standard protocols that utilize the Multi Gauge software (Fujifilm) to quantitate primer extension [41,44]. The results from dose response experiments were plotted using Prism 4 (GraphPad Software Inc., CA) and IC_{50} values for TFV-DP were obtained at midpoint concentrations.

ATP-dependent rescue assay

Template/primer (T_{31}/P_{18}) terminated with TFV (T/P_{TFV}) was prepared as described in Michailidis et al [41]. 20 nM of T/P_{TFV} was incubated at 37°C with HIV-1 RT (60 nM), either at various concentrations of ATP (0–7 mM) for 30 minutes, or for various times (0–120 minutes) with 3.5 mM ATP, in RT buffer containing 50 mM Tris-HCl, pH 7.8, and 50 mM NaCl, and 10 mM $MgCl_2$. The assay was performed in the presence of excess competing dATP (100 μM) that prevented reincorporation of the excised TFV, 0.5 μM dTTP and 10 μM ddGTP. Reactions were quenched with 100% formamide containing traces of bromophenol blue and analyzed as described above. The dissociation constants (K_d) of the various enzymes for ATP used in the rescue reactions were determined by fitting the rescue data at various ATP concentrations, using non-linear regression fitting to hyperbola.

Kinetics of dNTP incorporation by WT and mutant enzymes

To determine the binding affinity of WT and mutant enzymes to the dNTP substrate ($K_{D\text{-}dNTP}$) and to estimate the maximum rate of dNTP incorporation by these enzymes (k_{pol}), we carried out transient-state experiments using a rapid quench instrument (RQF-3, Kintek Corporation, Clarence, PA) at 37°C in RT buffer (50 mM Tris-HCl, pH 7.8 and 50 mM NaCl). HIV-1 RT (50 nM active sites) was pre-incubated with 50 nM T_{31}/P_{18} in one syringe (Syringe A), whereas varying concentrations of dNTP and 10 mM $MgCl_2$ were kept in another syringe (Syringe B). The solutions were rapidly mixed to initiate reactions, which were subsequently quenched at various times (5 ms to 10 s) by adding EDTA to a final concentration of 50 mM. The products from each quenched reaction were resolved, quantitated, and plotted as described above. The data were fit by non-linear regression to the burst equation (Eq 1).

To obtain the dissociation constant $K_{D\text{-}dNTP}$ for dNTP binding to the RT-DNA complex, the observed burst rates (k_{obs}) were fit to the hyperbolic equation (Eq. 3) using nonlinear regression:

$$k_{obs} = (k_{pol}[dNTP])/(K_{D-dNTP} + [dNTP]) \quad (3)$$

where k_{pol} is the optimal rate of dNTP incorporation.

The kinetics of TFV incorporation by the WT and mutant enzymes were carried out in a manner similar to that employed for natural dNTP substrate except the time of reactions. It was noted that the mutant enzymes required longer time to incorporate TFV compared to the WT HIV-1 RT (detailed in the Results section).

Molecular Modeling

Molecular models of mutant enzymes were generated using SYBYL (Tripos Associates, St. Louis, MO). The starting protein coordinates were from the crystal structure of HIV-1 RT in complex with DNA template/primer and TFV-DP (PDB file 1T05) [45]. They were initially modified by the Protein Preparation tool (Schrodinger Molecular Modeling Suit, NY), which deletes unwanted water molecules, sets charges and atom type of metal ions, corrects misoriented Gln and Asn residues, and optimizes H-atom orientations. Amino acid side chains were substituted in by Maestro (Schrodinger, Molecular Modeling Suite, NY). Molecular dynamics simulations of the WT and mutant RT models were carried out to obtain the most stable structures by Impact, interfaced with Maestro at constant temperature, and OPLS_2005 force field. The molecular dynamics simulations were performed for 1000 steps with 0.001 ps intervals. The temperature relaxation time was 0.01 ps. The Verlet integration algorithm was used in simulations. The structures were imported into Pymol (http://www.pymol.org) for visualization and comparison.

Results

Phenotypic resistance to TFV-DF in the absence of any known TFV resistance mutations

During phenotypic and genotypic evaluation of the clinical isolates we identified a unique virus that exhibited an apparent discordance between the phenotypic and genotypic results. The clinical history of the patient and the corresponding genotypic and phenotypic changes during the course of the therapy are summarized in Fig. 1. (Also see Table S1). The patient's treatment before Feb 2002 included d4T, ddI, and EFV and did not decrease significantly the viral loads (Fig 1A). Hence, the therapeutic regimen was switched to TFV-DF, EFV, and the protease inhibitor lopinavir (LPV). However, the patient's immunological and virological responses still did not improve due to poor adherence, especially to LPV. Genotypic and phenotypic analyses on March 2002 (point 1) and June 2002 (point 2) revealed

A

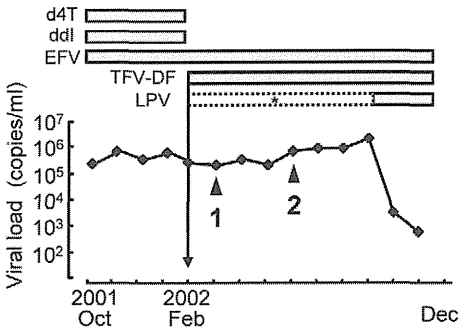

B Phenotypic profile

Isolate	Fold increase in EC_{50}								
	AZT	ddI	d4T	3TC	ABC	**TFV-DF**	FTC	NVP	EFV
1	61	12	9	13	10	**2**	9	>200	>500
2	57	>40	>50	31	15	**6**	5	>200	>500

C Genotypic profile

Isolate	Resistance-associated mutation		Other newly acquired mutations
	NRTI	NNRTI	
1	Q151M complex,	V106M, V179D	-
2	Q151M complex,	V106M, V179D, V108I	**K70Q**, K102R

Figure 1. Clinical course of patient and drug resistance profile. (A) The two clinical isolates were collected from the patient at the time points indicated by triangles. Both isolates had no known resistant mutations in the protease region. During the period indicated by asterisk, LPV was administrated but the patient demonstrated poor adherence due to undesirable side effects. After instruction on the use of antiretroviral drugs, the viral loads successfully decreased below the detection limit (<50 copies/ml). (B) Phenotypic drug susceptibility assays of clinical isolates in at least three independent experiments are shown as a relative increase in EC_{50} compared to HIV-1 NL4-3 strain which served as WT (see also Table S1). (C) Mutations observed in the isolates that are defined as the NRTI and NNRTI resistance associated mutations deposited in the HIV Drug Resistance Database maintained by International AIDS Society 2009 [58] and the Stanford University (http://hivdb.stanford.edu/) were shown. Abbreviations of drugs used: d4T, stavudine; ddI, didenosine; EFV, efavirenz; TFV-DF, tenofovir disoproxil fumarate; LPV, lopinovir; AZT, zidovudine; 3TC, lamivudine; ABC, abacavir; FTC, emtricitabine; NVP, nevirapine.
doi:10.1371/journal.pone.0016242.g001

resistance to multiple RT inhibitors, including NNRTIs (Fig 1B). Resistance to all NRTIs, except AZT and FTC, was enhanced in the point 2 isolate (Fig. 1B). Notably, this isolate showed an increase in resistance to TFV-DF in the absence of the canonical TFV resistance mutation (K65R) and in the presence of Q151Mc mutations (Fig. 1C). Previously, it has been shown that Q151Mc remains susceptible to TFV [22] although Smith *et al.* reported that Q151Mc had a 3.6-fold increase in TFV resistance [23]. Suppression of the viral load was finally achieved by improvement in drug adherence to LPV and by the addition of FTC in the therapeutic regimen, since no protease resistance mutations were found within the protease coding region.

To identify the mutation(s) responsible for the unexpected resistance to TFV-DF we sequenced the entire RT coding region at time-points 1 and 2 (Figure S1, GenBank Accession Number AB506802 and AB506803). Of the three substituted residues (70, 102, and 108) amino acids 102 and 108 are part of the structurally distinct NNRTI binding pocket [46], which can mutate during EFV-based therapeutic regimens. However, residue 70 is located in the β3-β4 hairpin loop of the p66 "fingers" subdomain of HIV-1 RT, which interacts with the incoming dNTP substrate [10,27]. Different mutations at this site have been previously implicated in NRTI resistance [47], suggesting that the observed K70Q mutation may be involved in the increased resistance to TFV-DF.

NRTI resistance enhancement by mutation at residue 70

Several mutations at position 70 of HIV-1 RT (R, G, E, T, N and Q) have been reported to the Stanford HIV-1 Drug Resistance Database (http://hivdb.stanford.edu/, accessed on Feb. 27th 2010). K70Q is rarely observed in treatment-naïve patients (0.04%), but appears more often in clinical samples from NRTI-treated patients (0.1%, $p<0.0001$ compared with the frequency of K70Q in treatment-naïve patients) but not NNRTI-treated patients. Furthermore, K70Q is observed in 0.5% of the clinical samples from patients infected with HIV-1 Q151M. There have been no previous reports on a possible role of K70Q in NRTI resistance.

To examine the effect of K70Q on drug susceptibility we generated a series of HIV variants with mutations at RT codon 70 (Figure 2A and also Table S2). The HIV-1_{K70Q} variant exhibited marginal resistance to ddI and 3TC (5- and 3.3-fold, respectively), but no significant resistance to other NRTIs. We further examined whether the mutations at residue 70 affect susceptibility to NRTIs in the Q151Mc background (Figure 2B and also Table S3). HIV-$1_{K70G/Q151Mc}$ had enhanced resistance to d4T (4.6-fold) as compared to HIV-1_{Q151Mc}. Notably, HIV-$1_{K70Q/Q151Mc}$ also showed enhanced resistance to ddI and d4T (2.4- and 4.4-fold, respectively, compared to HIV-1_{Q151Mc}). In addition, HIV-$1_{K70Q/Q151Mc}$ displayed 5-fold increased resistance to TFV-DF compared to HIV-1_{Q151Mc}. Other K70 mutations exhibited little or no resistance to TFV-DF.

Primer Extension and ATP-based Rescue Assays

As mentioned earlier, a key mechanism of NRTI resistance is the excision mechanism, which is based on the enhanced ability of NRTI-resistant enzymes to use ATP for unblocking chain-terminated primers and allow for further DNA synthesis to continue [2,3,48]. To determine whether the K70Q mutation causes TFV resistance through the excision mechanism we measured the susceptibility of WT and mutant RTs to inhibition by TFV in the presence or absence of ATP. In gel-based assays, an enhancement in excision would manifest as an increase in the production of fully extended DNA when 3.5 mM ATP is included in the extension reaction [49,50]. Our extension assays in the absence of ATP (no-excision conditions) showed that addition of the K70Q mutation to Q151Mc HIV-1 RT enhances resistance to TFV-DP. However, this enhancement is not influenced by the presence of ATP (Table 1, Fig. 3A and Figure S2A). In fact, excision enhancement due to the presence of ATP measured as [IC_{50} with ATP]/[IC_{50} without ATP] was similar for all enzymes, including the WT RT (from 2.7-fold to 2.9-fold for WT, K70Q, Q151Mc, and K70Q/Q151Mc RTs) (Table 1). Using a related type of assay, the ATP-mediated rescue assay, we compared the rates by which the WT and mutant RTs unblock TFV-terminated primers and extend products past the point of chain-termination. We find that the ATP-based rescue activity of WT RT is not slower, but 1.5-, 2.5-, and 3-fold faster than that of K70Q, Q151Mc, and K70Q/Q151Mc RTs, respectively (Fig. 3B and Figure S2B). In addition, the ATP-based rescue activity of WT RT was saturated at lower concentrations of ATP than K70Q,

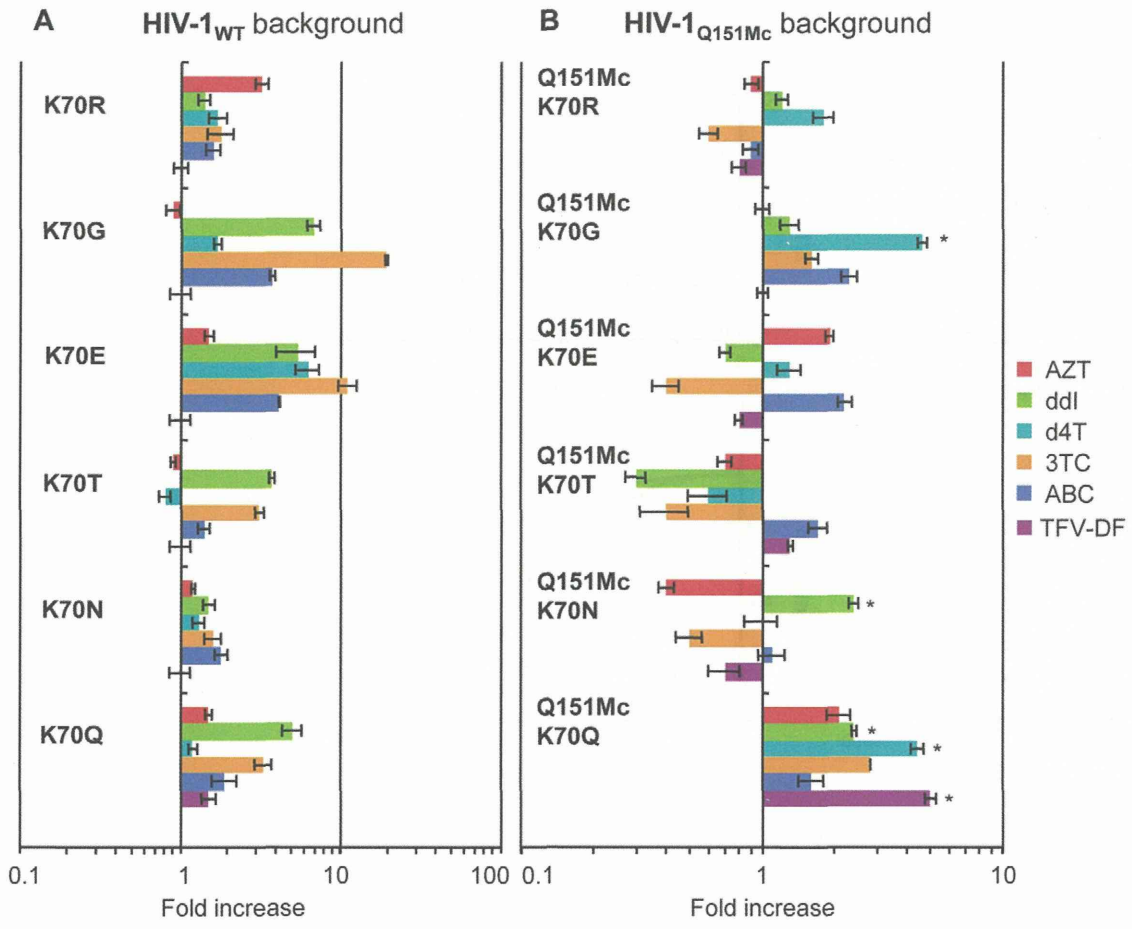

Figure 2. NRTI resistance of HIVs with mutations at RT residue 70 in the background of WT or Q151Mc. Antiviral activities of HIV-1s carrying mutations at residue 70 (K70R, K70G, K70E, K70T, K70N, or K70Q) in the WT (A) or Q151Mc (B) background were determined by the MAGIC5 assay. The data for each clone were compared to WT (A) and Q151Mc (B) HIV-1 and are shown as fold increase; AZT (red), ddI (green), d4T (cyan), 3TC (orange), ABC (blue), and TFV-DF (purple). Error bars represent standard deviations from at least three independent experiments (see also Table S2 and S3). The asterisk indicates statistically significant in EC_{50} values ($P<0.0001$ by t-test).
doi:10.1371/journal.pone.0016242.g002

Table 1. Primer extension assay in the presence or absence of ATP.

Enzyme[a]	IC_{50} (nM) of TFV-DP[b] (fold increase[c])		Excision enhancement due to ATP[d]
	Without ATP	**With ATP**	
WT	641±83	1854±197	2.9
	(1)[b]	(1)[b]	
K70Q	802±99	2306±270	2.9
	(1.3)	(1.2)	
Q151Mc	1503±90	3996±341	2.7
	(2.3)	(2.1)	
K70Q/Q151Mc	2392±353	7001±226	2.9
	(3.7)	**(3.8)**	

[a]The sequence of HIV RT WT and mutant derived from BH10.
[b]Data are means ± standard deviations from at least three independent experiments.
[c]The relative increase in IC_{50} value compared with each HIV-1 RT WT without, or with ATP is given in parentheses. Bold indicates an increase in fold increase value greater than 3-fold.
[d]Excision enhancement due to ATP is calculated as IC_{50} with ATP/IC_{50} without ATP.
doi:10.1371/journal.pone.0016242.t001

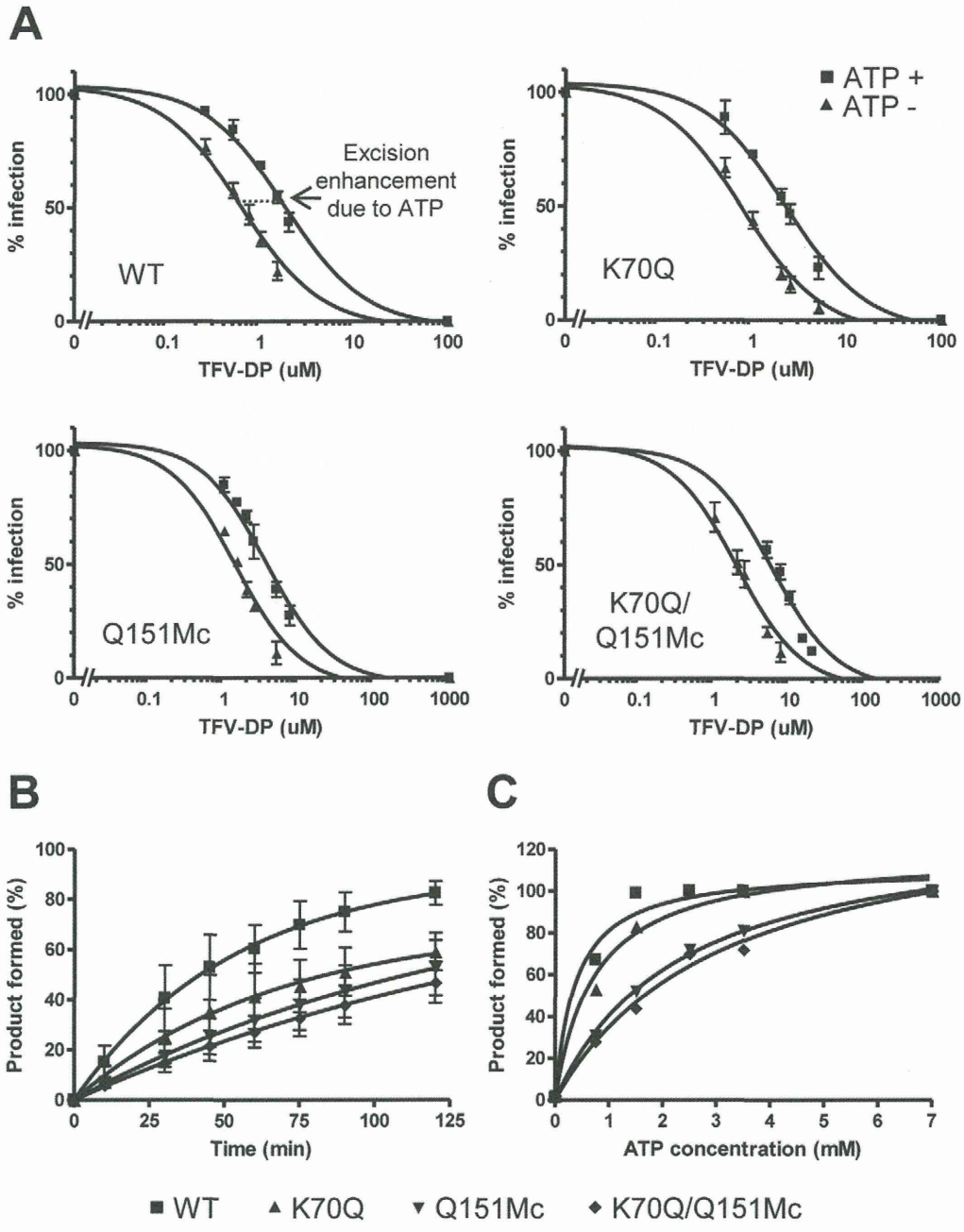

Figure 3. Effects of RT mutations K70Q, Q151Mc, or K70Q/Q151Mc on DNA primer extension activity and on ATP-based excision activities. (A) Effect of varying concentrations of TFV-DP on the primer extension activities of HIV-1 WT and mutant RTs. The experiments were carried out in the presence (■) or absence (▲) of 3.5 mM ATP (B) Time dependence of ATP-based rescue of TFV-terminated primers. TFV-terminated T_{31}/P_{18} oligos (20 nM) were incubated with 60 nM RT and 3.5 mM ATP. The reaction mixture also included excess of competing dATP (100 μM) that prevented reincorporation of TFV-DP and 0.5 μM dTTP, and 10 μM ddGTP that allowed extension of the rescued primer by two nucleotides and chain termination. Rescue products (WT [■], K70Q [▲], Q151Mc [▼] and K70Q/Q151Mc [♦]) were analyzed at indicated time points. (C) ATP-based rescue was dependent on concentration of ATP. Reactions were as in (B), but for 30 minutes and at varying concentrations of ATP. Rescue products at 7 mM ATP are defined as 100% product formed.
doi:10.1371/journal.pone.0016242.g003

Q151Mc, and K70Q/Q151Mc RTs (the apparent $K_{D\text{-}ATP}$ for WT, K70Q, Q151Mc and K70Q/Q151Mc were 0.4, 0.7, 2.3, and 3.1 mM, respectively), suggesting that a better binding of ATP may contribute to the slightly enhanced excision activity of WT RT (Fig. 3C and Figure S2C). Collectively, these results rule out the possibility that K70Q/Q151Mc becomes resistant to TFV through the excision mechanism.

Pre-Steady Kinetic Constants for Binding and Incorporation of dATP and TFV-DP

To determine whether the resistance by K70Q/Q151Mc is caused by an increased preference of physiological dATP substrate over TFV-DP, we carried out pre-steady state transient kinetic analyses of WT, K70Q, Q151Mc, and K70Q/Q151Mc enzymes. The kinetic constants $k_{pol\text{-}dATP}$ and $K_{D\text{-}dATP}$ for WT and mutant

enzymes are presented in Table 2 and Fig. 4 (and also in Figure S3). The results reveal that K70Q, Q151Mc, and K70Q/Q151Mc RTs have increased $k_{pol\text{-}dATP}$ as well as $K_{D\text{-}dATP}$. Both Q151Mc and K70Q/Q151Mc enzymes incorporate dATP faster than WT (17.9 and 14.6 s^{-1}, respectively *vs.* 6.3 s^{-1}) but have a weaker binding affinity for dATP than WT RT (5.4 and 5.0 μM, respectively *vs.* 2.6 μM). Hence, the catalytic efficiency ratio of dATP incorporation remains similar for all enzymes ($k_{pol\text{-}dATP}/K_{D\text{-}dATP}$ ratios for WT, K70Q, Q151Mc, and K70Q/Q151Mc were 2.4, 2.2, 3.3, and 2.9 $\mu M^{-1}\cdot s^{-1}$, respectively). On the contrary, a significant change in the incorporation efficiency of TFV was observed. The K70Q and K70Q/Q151Mc enzymes had more than 4.5-fold reduced affinity for TFV than the WT enzyme ($K_{D\text{-}TFV}$ values were 8.6 and 8.9 μM compared to 1.9 μM). In addition, the turnover rates of TFV incorporation by the WT and K70Q enzymes were comparable ($k_{pol\text{-}TFV}$ were 2.8 and 3.1 s^{-1}, respectively). The addition of the K70Q mutation to Q151Mc also reduced the k_{pol} for TFV-DP. The net effect of these changes was a significant reduction in the TFV-DP incorporation efficiencies of the mutant enzymes compared to the WT enzyme ($k_{pol\text{-}TFV}/K_{D\text{-}TFV}$ ratios for WT, K70Q, Q151Mc, and K70Q/Q151Mc were 1.47, 0.36, 0.3, and 0.11 $\mu M^{-1}\cdot s^{-1}$, respectively; Table 2). WT RT incorporated TFV-DP most efficiently, followed by K70Q>Q151Mc>K70Q/Q151Mc enzymes. As a direct measure of the enzyme's ability to discriminate between the natural dATP substrate and the TFV, we determined the "selectivity", defined as the ratio of efficiency of the enzyme to incorporate dATP over TFV-DP ($k_{pol\text{-}dATP}/K_{D\text{-}dATP}/k_{pol\text{-}TFV}/K_{D\text{-}TFV}$). The selectivity values demonstrate that the K70Q/Q151Mc enzyme favors incorporation of dNTP over TFV-DP 26.3 times compared to 1.6 times by the WT enzyme, leading to a 16.4-fold resistance to TFV (defined as $selectivity_{mutant}/selectivity_{WT}$; Table 2). This resistance is more than twice the TFV resistance of Q151Mc and 4 times the TFV resistance of K70Q.

Molecular modeling

Molecular dynamics simulations on the control structural coordinates of the WT RT/DNA/TFV-DP crystal structure [45] did not cause any significant structural changes, suggesting that the modeling protocols do not alter the structures in ways that are not related to the K70Q or Q151Mc mutations. The root mean square deviation (rmsd) between the Cα atoms of the WT structures before and after simulation was 0.1 Å. Similarly, the rmsd between the Cα atoms of WT and mutant RT molecular models were also very low (~0.1 Å). Comparison of these models showed a significant repositioning of residue 65 in Q151Mc/K70Q (Fig. 5), and to a lesser extent in K70Q or Q151Mc RTs (not shown). Additional smaller changes in the side chains of residues 151, 70, and 72 were also observed (Fig. 5). The structure of TFV-DP was also slightly adjusted, possibly as a result of the changes in the surrounding residues (Fig. 5). While residue 70 is located proximal to residue 65, and to the phosphates of the incoming TFV-DP, it does not appear to interact directly with these structural elements.

Discussion

We have discovered a novel HIV mutation that causes high-level resistance to TFV-DF. We have also determined the biochemical mechanism of this resistance. TFV-DF is a valuable NRTI therapeutic option for patients infected with multi-drug resistant Q151Mc HIV-1 [22]. We demonstrate here that Q151Mc can acquire an additional mutation, K70Q, which expands the multi-drug resistance to include high-level resistance to TFV-DF. We identified this mutant during genotypic analysis of clinical isolates from an HIV-infected patient who was not responding to TFV-DF. The K70Q/Q151Mc set of mutations is currently rare among HIV-infected patients. However, we believe that similar to K65R, its prevalence will increase, as tenofovir use continues to rise. Our virological studies with recombinant viruses confirmed that the observed enhancement and expansion of multi-drug resistance is the consequence of the addition of K70Q to Q151Mc HIV. Recently, the concept of clinical cut-offs (CCOs) has been introduced to improve the prediction of drug resistance during antiretroviral therapies. CCOs are better correlated with virologic response than biological cut-offs [51,52]. Importantly, K70Q/Q151Mc is 10 times less susceptible to TFV-DF than WT HIV-1, whereas the CCOs for TFV-DF is defined as a 2.1-fold reduction in virologic response to this inhibitor. Moreover, K70Q/Q151Mc is at least twice as resistant to TFV as the well-known TFV-resistant K65R in the background of Q151Mc (as reported in the Stanford HIV Drug Resistance Database).

Previous studies have offered insights into the drug resistance mechanism of similar mutations (K70E, K70G, K70R, and K70T). Specifically, K70E was selected in patients with virological failure after TFV-DF-based antiviral therapy [53,54,55]. K70T emerged in the background of Q151Mc during *in vitro* selection by TFV-DF [56]. K70R is a key mutation involved in resistance to AZT and appears in the background of other excision enhancement mutations [2,3,57]. In our case, a new mutation (K70Q) was

Table 2. Pre-steady state kinetic constants for binding and incorporation of dATP and TFV-DP by WT, K70Q, Q151Mc and K70Q/Q151Mc HIV-1 RT.

Pre-steady state kinetic constants[a]								
Enzyme[b]	dATP			TFV-DP			Selectivity[c]	Resistance[d]
	k_{pol} (s^{-1})	K_d (μM)	k_{pol}/K_d ($\mu M^{-1}\cdot s^{-1}$)	k_{pol} (s^{-1})	K_d (μM)	k_{pol}/K_d ($\mu M^{-1}\cdot s^{-1}$)		
WT	6.3±0.5	2.6±0.1	2.4±0.2	2.8±0.08	1.9±0.2	1.47±0.07	1.6	-
K70Q	8.4±0.4	3.8±0.6	2.2±0.4	3.1±0.4	8.6±1.5	0.36±0.08	6.1	3.8
Q151Mc	17.9±0.4	5.4±0.5	3.3±0.3	1.3±0.03	4.3±0.8	0.3±0.06	11	6.9
K70Q/Q151Mc	14.6±1.6	5.0±0.07	2.9±0.3	1.0±0.03	8.9±2.1	0.11±0.03	26.3	16.4

[a]Data are means ± standard deviations from at least three independent experiments.
[b]The sequence of HIV RT WT and mutant derived from BH10.
[c]Selectivity is defined as $(k_{pol}/K_d)_{dATP}/(k_{pol}/K_d)_{TFV\text{-}DP}$.
[d]Resistance (fold) is calculated as $selectivity_{mutant}/selectivity_{WT}$.
doi:10.1371/journal.pone.0016242.t002

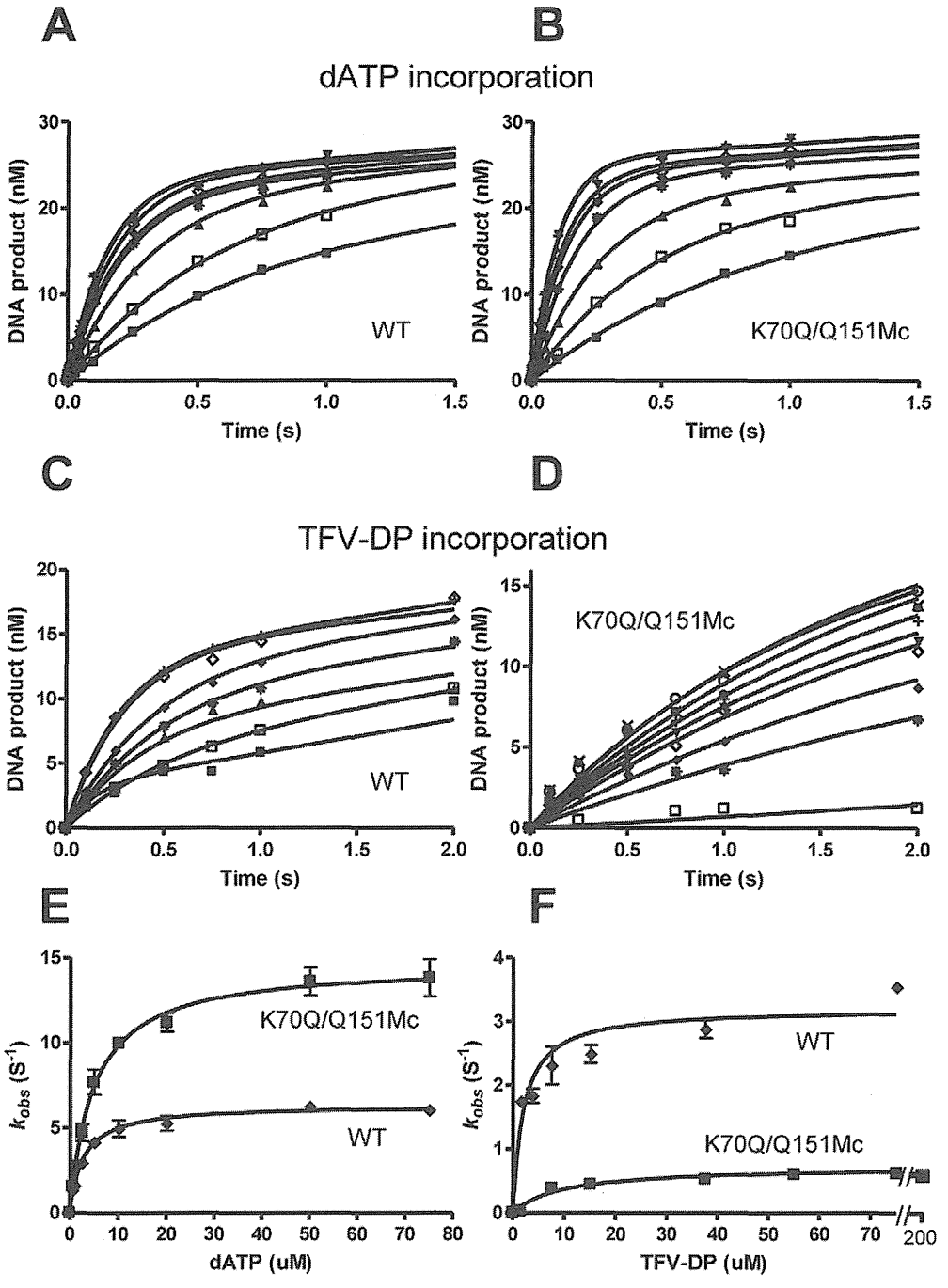

Figure 4. Pre-steady state kinetics of incorporation of dATP or TFV-DP by WT and K70Q/Q151Mc HIV-1 RTs. Single-nucleotide incorporation of dATP (panels A, B, and E) or TFV-DP (panels C, D, and F) by WT (panels A, C, E, and F) and K70Q/Q151Mc (panels B, D, E, and F). Formation of extended primer products in the reactions with WT RT and K70Q/Q151Mc RT were measured at 5 ms to 5 s time points, using the following dATP concentrations: 0.5 (■), 1 (□), 2.5 (▲), 5 (*), 10 (♦), 20 (◇), 50 (▼) and 75 μM (+). Incorporation of TFV was measured at 0.1–10 s reactions and at the following TFV-DP concentrations: 0.75 (■), 1.5 (□), 3.75 (▲), 7.5 (*), 15 (♦), 37.5 (◇) and 75 μM (+) for reactions with WT RT (panel C), and 1.5 (□), 7.5 (*), 15 (♦), 37.5 (◇), 55 (▼), 75 (+), 112.5 (•), 150 (○) and 200 μM (x) for reactions with K70Q/Q151Mc RT (panel D). (E) The amplitudes of the burst phases from the dATP reactions shown in panels A (WT, [♦]) and B (K70Q/Q151Mc, [■]) were plotted as a function of dATP concentrations. (F) The amplitudes of the burst phases from the TFV-DP reactions shown in panels C (WT, [♦]) and D (K70Q/Q151Mc, [■]) were plotted as a function of TFV-DP concentrations. The solid lines in panels A, B, C, and D represent the best fit of data to the burst equation. Each point represents the average values of three experiments.
doi:10.1371/journal.pone.0016242.g004

identified in a patient infected with Q151Mc HIV-1 during the course of TFV-DF-based antiviral therapy. The International AIDS Society-USA publishes [58] every year a list of HIV-1 drug resistance mutations compiled by a panel of experts charged with the goal of delivering accurate, unbiased, and evidence-based information for use by HIV clinical practitioners. In order for a novel mutation to be accepted in the list it should meet at least *one* of the following criteria: 1) *in vitro* passage experiments or

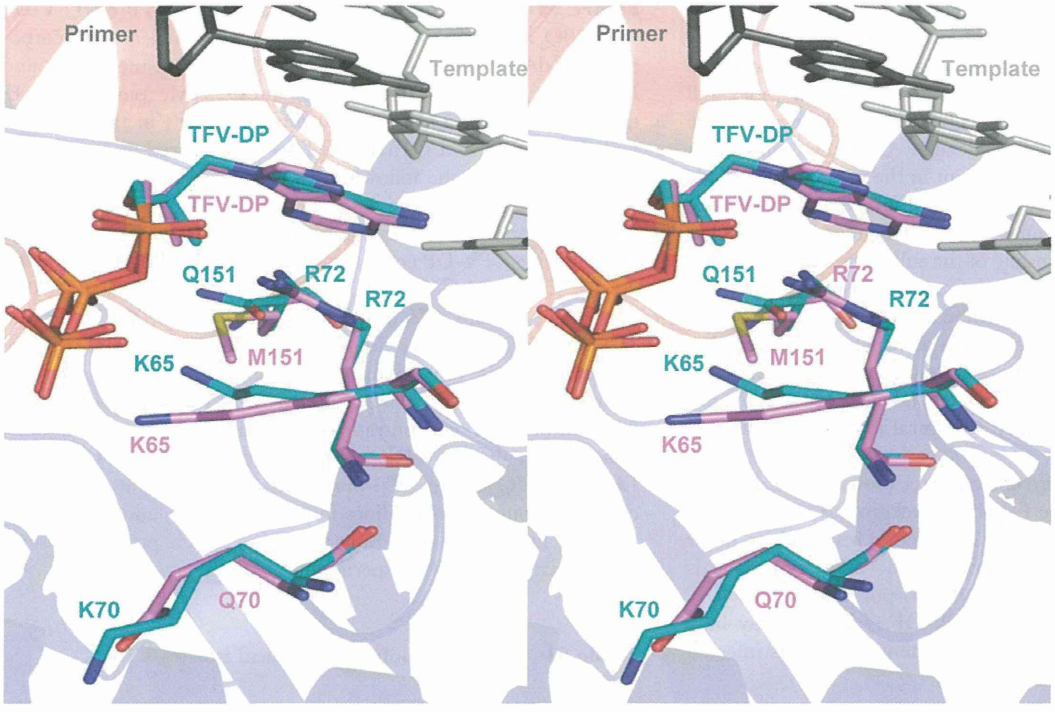

Figure 5. Stereo view of TFV-DP in the polymerase active site of WT RT and K70Q/Q151Mc RT. WT RT residues are shown as cyan sticks, K70Q/Q151Mc RT residues are shown as purple sticks. The primer strand is shown as dark gray sticks, template strand as light gray sticks. The fingers and palm subdomains are shown as blue and red cartoons, respectively.
doi:10.1371/journal.pone.0016242.g005

validation of contribution to resistance by using site-directed mutagenesis; 2) susceptibility testing of laboratory or clinical isolates; 3) nucleotide sequencing of viruses from patients in whom the drug is failing; 4) correlation studies between genotype at baseline and virologic response in patients exposed to a drug. Our study has unambiguously demonstrated that K70Q meets at least the first three criteria: evidence for criterion #1 is shown in Figure 2; for criterion #2 in Figures 1 and 2; and for criterion #3 in Figure 1 and Figure S1. Therefore, the K70Q mutation meets the criteria of a clinically relevant mutation.

In addition to the clinical and virological studies, we used biochemical techniques to determine the mechanism of TFV resistance imparted by the K70Q mutation to Q151Mc RTs. We used primer extension assays to show that K70Q/Q151Mc RT is less susceptible to TFV-DP than WT and Q151Mc RTs. We demonstrated that the mechanism of this resistance is not based on excision. On the contrary, we showed that the ATP-based excision of the mutant enzymes was slightly decreased with respect to WT RT, possibly because of decreased affinity of the mutant enzymes for the ATP excision substrate, incurred by changes in the binding environment of ATP, such as the loss of lysine at position 70.

Using transient-state kinetics we unambiguously established that the overall mechanism of K70Q/Q151Mc resistance to TFV is due to enhanced discrimination between the natural dATP substrate and TFV-DP. While all mutant enzymes had comparable efficiency of dATP incorporation, they displayed varying affinity and turnover rates of incorporation. It appears that the stronger effect of the enhanced discrimination overcomes the slight increase in sensitivity due to the small increase in excision. As a result, the mutant enzymes are resistant to the inhibitor.

Mutations at position 70 of RT have been known to confer NRTI resistance by two distinct mechanisms: K70R combined with at least two excision enhancing mutations, D67N and T215Y, enhances ATP-mediated excision of AZT and d4T [1,2,3,48] (*excision–dependent mechanism*). On the other hand, K70E causes resistance to 3TC, TFV, and ABC by lowering the maximum rate of inhibitor incorporation by RT (k_{pol}*-dependent exclusion mechanism*) [55]. Our results establish that in the background of Q151Mc, K70Q causes TFV resistance through a third mechanism: by decreasing the binding affinity of the inhibitor (K_d*-dependent exclusion mechanism*). Taken together, these findings highlight the remarkable ability of RT to use separate mutations at a single position to acquire NRTI resistance through three different mechanisms.

Our cell-based assays with infectious HIV-1 show that Q151Mc remains susceptible to TFV-DF, a finding consistent with previous reports [22]. Similarly, clinical isolates deposited at the Stanford HIV resistance database and carrying the Q151Mc mutation were also susceptible to TFV-DF, unless they also had the K65R mutation. However, pre-steady state characterization of TFV-DP incorporation by Q151Mc in this work (Table 2) and by others [59] showed that Q151Mc is less susceptible to TFV-DP than WT RT. This small discrepancy may be the result of potential differences in DNA-dependent and RNA-dependent DNA synthesis, or the result of the slightly increased excision of Q151Mc RT compared to WT RT (Fig. 3B and C).

To gain insights into the possible structural changes caused by the addition of K70Q to Q151Mc, we compared the molecular model of K70Q/Q151Mc RT/DNA/TFV-DP with the crystal structure of WT RT/DNA/TFV-DP [45] (Fig. 5). The network of hydrogen bonds involving the side-chains of K65, R72, and Q151 in the WT structure [26,27,54], is disrupted in the mutant structure. Also, Q151M and associated mutations A62V, V75I, and F77L are likely to modify the hydrophobic core of the fingers. We and others have previously shown that the side-chains of residues 72 and 65 interact with each other [35] and with Q151

and the α- and γ-phosphates of the incoming dNTP [26] or TFV-DP [45]. The functions of these residues have been established by several biochemical studies [21,25,60,61,62,63]. The reduction in polymerase rate (k_{pol}) and in binding affinity for TFV-DP (increased $K_{d,TFV\text{-}DP}$) may be the consequence of one or more such structural changes. Our molecular dynamics simulation experiments suggested a re-arrangement in the position of the side chain of K65, which is a catalytically important residue. While the precise effect of this change is not clear at this point, such changes could influence the overall binding of the substrate and/or the rate of nucleotide incorporation. Moreover, such movement of K65 in the presence of a mutation at position 70 is consistent with our previously reported crystallographic data, which established that there is an interplay between the positioning of the side chains at positions 70 and 65 [64]. Ongoing crystallographic studies are expected to provide more detailed structural insights into the role of K70Q in drug resistance.

In summary, we report here clinical data showing that addition of the K70Q mutation to the Q151Mc background confers high-level HIV resistance to TFV-DF and enhances resistance to other NRTIs. The biochemical mechanism of the TFV resistance is based on reduced binding affinity and incorporation of TFV-DP. Detection of this novel pattern of TFV-DF resistance may help adjust therapeutic regimens for the treatment of patients infected with multi-drug resistant HIV-1.

Supporting Information

Figure S1 Amino acid sequence alignment of the RT regions (amino acid 32 to 560) of the clinical isolates at time points 1 to 2 (see Figure 1A).
(DOC)

Figure S2 Effects of RT mutations K70Q, Q151Mc, or K70Q/Q151Mc on DNA primer extension activity and on ATP-based excision activities. (A) Effect of varying concentrations of TFV-DP on the primer extension activities of HIV-1 WT and mutant RTs. The experiments were carried out in the presence and absence of 3.5 mM ATP (marked as ATP (+) and ATP (−), respectively). Addition of ATP in the polymerization mixture allows measurement of the net sum of DNA polymerization and ATP-based excision activities. (B) Time dependence of ATP-based rescue of TFV-terminated primers. (C) ATP-based rescue was dependent on concentration of ATP.
(PPTX)

Figure S3 Pre-steady state incorporation of dATP or TFV-DP by K70Q and Q151Mc HIV-1 RTs. Single-nucleotide incorporation of dATP (panels A, B, and E) or TFV-DP (panels C, D, and F) by K70Q (panels A, C, E, and F) and Q151Mc (panels B, D, E, and F). Formation of extended primer products in the reactions with K70Q RT and Q151Mc RT were measured at 5 ms to 5 s time points, using the following dATP concentrations: 0.5 (■), 1 (□), 2.5 (▲), 5 (*), 10 (♦), 20 (◇), 50 (▼) and 75 μM (+). Incorporation of TFV was measured at 0.1–10 s reactions and at the following TFV-DP concentrations: 0.75 (■), 1.5 (□), 3.75 (▲), 7.5 (*), 15 (♦), 37.5 (◇) and 75 μM (▼) for reactions with K70Q RT (panel C), and 3.75 (▲), 7.5 (*), 37.5 (◇), 55 (▼), 75 (+) and 112.5 (•) for reactions with Q151Mc RT (panel D). (E) The amplitudes of the burst phases from the dATP reactions shown in panels A (K70Q, [▲]) and B (Q151Mc, [▼]) were plotted as a function of dATP concentrations. (F) The amplitudes of the burst phases from the TFV-DP reactions shown in panels C (K70Q, [▲]) and D (Q151Mc, [▼]) were plotted as a function of TFV-DP concentrations. The solid lines in panels A, B, C, and D represent the best fit of data to a burst equation. Each point represents average values of three experiments.
(PPTX)

Table S1 Drug susceptibility of clinical isolates.
(DOC)

Table S2 Drug susceptibility of HIV-1 variants carrying mutation at residue 70.
(DOC)

Table S3 Drug susceptibility of HIV-1 variants carrying mutation at residue 70 in the background of Q151M complex.
(DOC)

Acknowledgments

We thank Yukiko Takahashi and Fujie Negishi for sample preparation, and Dr. Hiroyuki Gatanaga and Dr. Michael A. Parniak for helpful discussions.

Author Contributions

Conceived and designed the experiments: AH ENK SO SGS. Performed the experiments: AH MMS KAK EM YS KS. Analyzed the data: AH MMS KAK KS SGS. Contributed reagents/materials/analysis tools: AH ENK SGS OS. Wrote the paper: AH ENK KS SGS.

References

1. Meyer PR, Matsuura SE, Mian AM, So AG, Scott WA (1999) A mechanism of AZT resistance: an increase in nucleotide-dependent primer unblocking by mutant HIV-1 reverse transcriptase. Mol Cell 4: 35–43.
2. Boyer PL, Sarafianos SG, Arnold E, Hughes SH (2001) Selective excision of AZTMP by drug-resistant human immunodeficiency virus reverse transcriptase. J Virol 75: 4832–4842.
3. Arion D, Kaushik N, McCormick S, Borkow G, Parniak MA (1998) Phenotypic mechanism of HIV-1 resistance to 3′-azido-3′-deoxythymidine (AZT): increased polymerization processivity and enhanced sensitivity to pyrophosphate of the mutant viral reverse transcriptase. Biochemistry 37: 15908–15917.
4. Singh K, Marchand B, Kirby KA, Michailidis E, Sarafianos SG (2010) Structural aspects of drug resistance and inhibition of HIV-1 reverse transcriptase. Viruses 2: 606–638.
5. Mas A, Parera M, Briones C, Soriano V, Martinez MA, et al. (2000) Role of a dipeptide insertion between codons 69 and 70 of HIV-1 reverse transcriptase in the mechanism of AZT resistance. EMBO J 19: 5752–5761.
6. Matamoros T, Franco S, Vazquez-Alvarez BM, Mas A, Martinez MA, et al. (2004) Molecular determinants of multi-nucleoside analogue resistance in HIV-1 reverse transcriptases containing a dipeptide insertion in the fingers subdomain: effect of mutations D67N and T215Y on removal of thymidine nucleotide analogues from blocked DNA primers. J Biol Chem 279: 24569–24577.
7. Meyer PR, Lennerstrand J, Matsuura SE, Larder BA, Scott WA (2003) Effects of dipeptide insertions between codons 69 and 70 of human immunodeficiency virus type 1 reverse transcriptase on primer unblocking, deoxynucleoside triphosphate inhibition, and DNA chain elongation. J Virol 77: 3871–3877.
8. Kew Y, Olsen LR, Japour AJ, Prasad VR (1998) Insertions into the beta3-beta4 hairpin loop of HIV-1 reverse transcriptase reveal a role for fingers subdomain in processive polymerization. J Biol Chem 273: 7529–7537.
9. Boyer PL, Sarafianos SG, Arnold E, Hughes SH (2002) Nucleoside analog resistance caused by insertions in the fingers of human immunodeficiency virus type 1 reverse transcriptase involves ATP-mediated excision. J Virol 76: 9143–9151.
10. Menendez-Arias L (2008) Mechanisms of resistance to nucleoside analogue inhibitors of HIV-1 reverse transcriptase. Virus Res 134: 124–146.
11. Sarafianos SG, Marchand B, Das K, Himmel DM, Parniak MA, et al. (2009) Structure and function of HIV-1 reverse transcriptase: molecular mechanisms of polymerization and inhibition. J Mol Biol 385: 693–713.
12. Sarafianos SG, Das K, Clark AD, Jr., Ding J, Boyer PL, et al. (1999) Lamivudine (3TC) resistance in HIV-1 reverse transcriptase involves steric hindrance with beta-branched amino acids. Proc Natl Acad Sci U S A 96: 10027–10032.
13. Gao HQ, Boyer PL, Sarafianos SG, Arnold E, Hughes SH (2000) The role of steric hindrance in 3TC resistance of human immunodeficiency virus type-1 reverse transcriptase. J Mol Biol 300: 403–418.

14. Shafer RW, Kozal MJ, Winters MA, Iversen AK, Katzenstein DA, et al. (1994) Combination therapy with zidovudine and didanosine selects for drug-resistant human immunodeficiency virus type 1 strains with unique patterns of pol gene mutations. J Infect Dis 169: 722–729.
15. Shirasaka T, Kavlick MF, Ueno T, Gao WY, Kojima E, et al. (1995) Emergence of human immunodeficiency virus type 1 variants with resistance to multiple dideoxynucleosides in patients receiving therapy with dideoxynucleosides. Proc Natl Acad Sci U S A 92: 2398–2402.
16. Iversen AK, Shafer RW, Wehrly K, Winters MA, Mullins JI, et al. (1996) Multidrug-resistant human immunodeficiency virus type 1 strains resulting from combination antiretroviral therapy. J Virol 70: 1086–1090.
17. Maeda Y, Venzon DJ, Mitsuya H (1998) Altered drug sensitivity, fitness, and evolution of human immunodeficiency virus type 1 with pol gene mutations conferring multi-dideoxynucleoside resistance. J Infect Dis 177: 1207–1213.
18. Matsumi S, Kosalaraksa P, Tsang H, Kavlick MF, Harada S, et al. (2003) Pathways for the emergence of multi-dideoxynucleoside-resistant HIV-1 variants. AIDS 17: 1127–1137.
19. Kosalaraksa P, Kavlick MF, Maroun V, Le R, Mitsuya H (1999) Comparative fitness of multi-dideoxynucleoside-resistant human immunodeficiency virus type 1 (HIV-1) in an In vitro competitive HIV-1 replication assay. J Virol 73: 5356–5363.
20. Garcia Lerma J, Schinazi RF, Juodawlkis AS, Soriano V, Lin Y, et al. (1999) A rapid non-culture-based assay for clinical monitoring of phenotypic resistance of human immunodeficiency virus type 1 to lamivudine (3TC). Antimicrob Agents Chemother 43: 264–270.
21. Feng JY, Myrick F, Selmi B, Deval J, Canard B, et al. (2005) Effects of HIV Q151M-associated multi-drug resistance mutations on the activities of (-)-beta-D-1′,3′-dioxolan guanine. Antiviral Res 66: 153–158.
22. Miller MD, Margot NA, Hertogs K, Larder B, Miller V (2001) Antiviral activity of tenofovir (PMPA) against nucleoside-resistant clinical HIV samples. Nucleosides Nucleotides Nucleic Acids 20: 1025–1028.
23. Smith RA, Gottlieb GS, Anderson DJ, Pyrak CL, Preston BD (2008) Human immunodeficiency virus types 1 and 2 exhibit comparable sensitivities to Zidovudine and other nucleoside analog inhibitors in vitro. Antimicrob Agents Chemother 52: 329–332.
24. Ueno T, Shirasaka T, Mitsuya H (1995) Enzymatic characterization of human immunodeficiency virus type 1 reverse transcriptase resistant to multiple 2′,3′-dideoxynucleoside 5′-triphosphates. J Biol Chem 270: 23605–23611.
25. Deval J, Selmi B, Boretto J, Egloff MP, Guerreiro C, et al. (2002) The molecular mechanism of multidrug resistance by the Q151M human immunodeficiency virus type 1 reverse transcriptase and its suppression using alpha-boranophosphate nucleotide analogues. J Biol Chem 277: 42097–42104.
26. Huang H, Chopra R, Verdine GL, Harrison SC (1998) Structure of a covalently trapped catalytic complex of HIV-1 reverse transcriptase: implications for drug resistance. Science 282: 1669–1675.
27. Sarafianos SG, Das K, Hughes SH, Arnold E (2004) Taking aim at a moving target: designing drugs to inhibit drug-resistant HIV-1 reverse transcriptases. Curr Opin Struct Biol 14: 716–730.
28. Gu Z, Fletcher RS, Arts EJ, Wainberg MA, Parniak MA (1994) The K65R mutant reverse transcriptase of HIV-1 cross-resistant to 2′, 3′-dideoxycytidine, 2′,3′-dideoxy-3′-thiacytidine, and 2′,3′-dideoxyinosine shows reduced sensitivity to specific dideoxynucleoside triphosphate inhibitors in vitro. J Biol Chem 269: 28118–28122.
29. Winters MA, Shafer RW, Jellinger RA, Mamtora G, Gingeras T, et al. (1997) Human immunodeficiency virus type 1 reverse transcriptase genotype and drug susceptibility changes in infected individuals receiving dideoxyinosine monotherapy for 1 to 2 years. Antimicrob Agents Chemother 41: 757–762.
30. Harrigan PR, Stone C, Griffin P, Najera I, Bloor S, et al. (2000) Resistance profile of the human immunodeficiency virus type 1 reverse transcriptase inhibitor abacavir (1592U89) after monotherapy and combination therapy. CNA2001 Investigative Group. J Infect Dis 181: 912–920.
31. Margot NA, Isaacson E, McGowan I, Cheng AK, Schooley RT, et al. (2002) Genotypic and phenotypic analyses of HIV-1 in antiretroviral-experienced patients treated with tenofovir DF. AIDS 16: 1227–1235.
32. Sluis-Cremer N, Arion D, Kaushik N, Lim H, Parniak MA (2000) Mutational analysis of Lys65 of HIV-1 reverse transcriptase. Biochem J 348 Pt 1: 77–82.
33. Deval J, Navarro JM, Selmi B, Courcambeck J, Boretto J, et al. (2004) A loss of viral replicative capacity correlates with altered DNA polymerization kinetics by the human immunodeficiency virus reverse transcriptase bearing the K65R and L74V dideoxynucleoside resistance substitutions. J Biol Chem 279: 25489–25496.
34. Feng JY, Myrick FT, Margot NA, Mulamba GB, Rimsky L, et al. (2006) Virologic and enzymatic studies revealing the mechanism of K65R- and Q151M-associated HIV-1 drug resistance towards emtricitabine and lamivudine. Nucleosides Nucleotides Nucleic Acids 25: 89–107.
35. Das K, Bandwar RP, White KL, Feng JY, Sarafianos SG, et al. (2009) Structural basis for the role of the K65r mutation in HIV-1 reverse transcriptase polymerization, excision antagonism, and tenofovir resistance. J Biol Chem 284: 35092–35100.
36. McColl DJ, Miller MD (2003) The use of tenofovir disoproxil fumarate for the treatment of nucleoside-resistant HIV-1. J Antimicrob Chemother 51: 219–223.
37. Chappell BJ, Margot NA, Miller MD (2007) Long-term follow-up of patients taking tenofovir DF with low-level HIV-1 viremia and the K65R substitution in HIV-1 RT. AIDS 21: 761–763.
38. Hachiya A, Kodama EN, Sarafianos SG, Schuckmann MM, Sakagami Y, et al. (2008) Amino acid mutation N348I in the connection subdomain of human immunodeficiency virus type 1 reverse transcriptase confers multiclass resistance to nucleoside and nonnucleoside reverse transcriptase inhibitors. J Virol 82: 3261–3270.
39. Shimura K, Kodama E, Sakagami Y, Matsuzaki Y, Watanabe W, et al. (2008) Broad antiretroviral activity and resistance profile of the novel human immunodeficiency virus integrase inhibitor elvitegravir (JTK-303/GS-9137). J Virol 82: 764–774.
40. Hachiya A, Aizawa-Matsuoka S, Tanaka M, Takahashi Y, Ida S, et al. (2001) Rapid and simple phenotypic assay for drug susceptibility of human immunodeficiency virus type 1 using CCR5-expressing HeLa/CD4(+) cell clone 1-10 (MAGIC-5). Antimicrob Agents Chemother 45: 495–501.
41. Michailidis E, Marchand B, Kodama EN, Singh K, Matsuoka M, et al. (2009) Mechanism of inhibition of HIV-1 reverse transcriptase by 4′-Ethynyl-2-fluoro-2′-deoxyadenosine triphosphate, a translocation-defective reverse transcriptase inhibitor. J Biol Chem 284: 35681–35691.
42. Singh K, Srivastava A, Patel SS, Modak MJ (2007) Participation of the fingers subdomain of Escherichia coli DNA polymerase I in the strand displacement synthesis of DNA. J Biol Chem 282: 10594–10604.
43. Kati WM, Johnson KA, Jerva LF, Anderson KS (1992) Mechanism and fidelity of HIV reverse transcriptase. J Biol Chem 267: 25988–25997.
44. Schuckmann MM, Marchand B, Hachiya A, Kodama EN, Kirby KA, et al. The N348I mutation at the connection subdomain of HIV-1 reverse transcriptase decreases binding to nevirapine. J Biol Chem.
45. Tuske S, Sarafianos SG, Clark AD, Jr., Ding J, Naeger LK, et al. (2004) Structures of HIV-1 RT-DNA complexes before and after incorporation of the anti-AIDS drug tenofovir. Nat Struct Mol Biol 11: 469–474.
46. Ren J, Nichols CE, Chamberlain PP, Weaver KL, Short SA, et al. (2004) Crystal structures of HIV-1 reverse transcriptases mutated at codons 100, 106 and 108 and mechanisms of resistance to non-nucleoside inhibitors. J Mol Biol 336: 569–578.
47. Clark S, Calef C, J M (2006) Mutations in Retroviral Genes Associated with Drug Resistance. HIV Sequence Compendium 2005: 58–175.
48. Meyer PR, Matsuura SE, So AG, Scott WA (1998) Unblocking of chain-terminated primer by HIV-1 reverse transcriptase through a nucleotide-dependent mechanism. Proc Natl Acad Sci U S A 95: 13471–13476.
49. Rigourd M, Ehresmann C, Parniak MA, Ehresmann B, Marquet R (2002) Primer unblocking and rescue of DNA synthesis by azidothymidine (AZT)-resistant HIV-1 reverse transcriptase: comparison between initiation and elongation of reverse transcription and between (−) and (+) strand DNA synthesis. J Biol Chem 277: 18611–18618.
50. Frankel FA, Marchand B, Turner D, Gotte M, Wainberg MA (2005) Impaired rescue of chain-terminated DNA synthesis associated with the L74V mutation in human immunodeficiency virus type 1 reverse transcriptase. Antimicrob Agents Chemother 49: 2657–2664.
51. Winters B, Montaner J, Harrigan PR, Gazzard B, Pozniak A, et al. (2008) Determination of clinically relevant cutoffs for HIV-1 phenotypic resistance estimates through a combined analysis of clinical trial and cohort data. J Acquir Immune Defic Syndr 48: 26–34.
52. Van Houtte M, Picchio G, Van Der Borght K, Pattery T, Lecocq P, et al. (2009) A comparison of HIV-1 drug susceptibility as provided by conventional phenotyping and by a phenotype prediction tool based on viral genotype. J Med Virol 81: 1702–1709.
53. Delaugerre C, Flandre P, Marcelin AG, Descamps D, Tamalet C, et al. (2008) National survey of the prevalence and conditions of selection of HIV-1 reverse transcriptase K70E mutation. J Med Virol 80: 762–765.
54. Kagan RM, Lee TS, Ross L, Lloyd RM, Jr., Lewinski MA, et al. (2007) Molecular basis of antagonism between K70E and K65R tenofovir-associated mutations in HIV-1 reverse transcriptase. Antiviral Res 75: 210–218.
55. Sluis-Cremer N, Sheen CW, Zelina S, Torres PS, Parikh UM, et al. (2007) Molecular mechanism by which the K70E mutation in human immunodeficiency virus type 1 reverse transcriptase confers resistance to nucleoside reverse transcriptase inhibitors. Antimicrob Agents Chemother 51: 48–53.
56. Van Laethem K, Pannecouque C, Vandamme AM (2007) Mutations at 65 and 70 within the context of a Q151M cluster in human immunodeficiency virus type 1 reverse transcriptase impact the susceptibility to the different nucleoside reverse transcriptase inhibitors in distinct ways. Infect Genet Evol 7: 600–603.
57. Larder BA, Kemp SD (1989) Multiple mutations in HIV-1 reverse transcriptase confer high-level resistance to zidovudine (AZT). Science 246: 1155–1158.
58. Johnson VA, Brun-Vezinet F, Clotet B, Gunthard HF, Kuritzkes DR, et al. (2009) Update of the drug resistance mutations in HIV-1: December 2009. Top HIV Med 17: 138–145.
59. Frangeul A, Bussetta C, Deval J, Barral K, Alvarez K, et al. (2008) Gln151 of HIV-1 reverse transcriptase acts as a steric gate towards clinically relevant acyclic phosphonate nucleotide analogues. Antivir Ther 13: 115–124.
60. Garforth SJ, Kim TW, Parniak MA, Kool ET, Prasad VR (2007) Site-directed mutagenesis in the fingers subdomain of HIV-1 reverse transcriptase reveals a specific role for the beta3-beta4 hairpin loop in dNTP selection. J Mol Biol 365: 38–49.
61. Sarafianos SG, Pandey VN, Kaushik N, Modak MJ (1995) Glutamine 151 participates in the substrate dNTP binding function of HIV-1 reverse transcriptase. Biochemistry 34: 7207–7216.

62. Frangeul A, Barral K, Alvarez K, Canard B (2007) In vitro suppression of K65R reverse transcriptase-mediated tenofovir- and adefovir-5′-diphosphate resistance conferred by the boranophosphonate derivatives. Antimicrob Agents Chemother 51: 3162–3167.
63. Sarafianos SG, Pandey VN, Kaushik N, Modak MJ (1995) Site-directed mutagenesis of arginine 72 of HIV-1 reverse transcriptase. Catalytic role and inhibitor sensitivity. J Biol Chem 270: 19729–19735.
64. Tu X, Das K, Han Q, Bauman JD, Clark AD, Jr., et al. Structural basis of HIV-1 resistance to AZT by excision. Nat Struct Mol Biol 17: 1202–1209.

INTERNAL MEDICINE

□ ORIGINAL ARTICLE □

Open-Label Randomized Multicenter Selection Study of Once Daily Antiretroviral Treatment Regimen Comparing Ritonavir-Boosted Atazanavir to Efavirenz with Fixed-Dose Abacavir and Lamivudine

Miwako Honda[1], Michiyo Ishisaka[1], Naoki Ishizuka[2], Satoshi Kimura[3], Shinichi Oka[1] and behalf of Japanese Anti-HIV-1 QD Therapy Study Group

Abstract

Background The side-effects of anti-retroviral drugs are different between Japanese and Caucasian patients. Severe central nerve system (CNS) side-effects to efavirenz and low rate of hypersensitivity against abacavir characterize the Japanese.

Objective The objective of this study was to select a once daily regimen for further non-inferior study comparing the virological efficacy and safety of the first line once daily antiretroviral treatment regimens in the current HIV/AIDS guideline.

Methods The study design was a randomized, open label, multicenter, selection study. One arm was treated with efavirenz and the other with ritonavir-boosted atazanavir. A fixed-dose lamivudine plus abacavir were used in both arms. The primary endpoint was virologic success (viral load less than 50 copies/mL) rate at 48 weeks. Patients were followed-up to 96 weeks with safety as the secondary endpoint. Clinicaltrials.Gov (NCT 00280969) and the University hospital Medical Information Network (UMIN000000243).

Results A total of 71 participants were enrolled. Virologic success rates in both arms were similar at week 48 [efavirenz arm 28/36 (77.8%); atazanavir arm 27/35 (77.1%)], but were decreased at week 96 to 55.6% in the efavirenz arm and 68.8% in the atazanavir arm (p=0.33). At the 96-week follow-up, 52.8% of the EFV arm and 34.3% of the ATV/r arm reached total cholesterol more than 220 mg/dL and required treatment. None of the patients developed cardiovascular complications in this study by week 96.

Conclusion There was no significant difference in the efficacy of efavirenz and ritonavir-boosted atazanavir combined with lamivudine plus abacavir at 48 weeks. The evaluation of safety was extended to 96 weeks, which also showed no significant difference in both arms.

Key words: HIV, antiretroviral treatment, efavirenz, atazanavir, abacavir, lamivudine

(Intern Med 50: 699-705, 2011)
(DOI: 10.2169/internalmedicine.50.4572)

Introduction

The use of a non-nucleoside transcriptase inhibitor (NNRTI) or ritonavir-boosted protease inhibitor as the key drug, combined with two nucleoside reverse-transcriptase inhibitors (NRTI), as the backbone drugs, is recommended as an initial therapy in human immunodeficiency virus type 1 (HIV-1) infection. For the key drug, when efavirenz (EFV) or ritonavir-boosted atazanavir (ATV/r) is selected, once daily therapy is possible. EFV is a widely used NNRTI, however, in some clinical studies conducted in Asia, a higher rate of adverse events, especially central nervous system-related symptoms, has been noted (1-3).

In terms of backbone drugs, didanosine (ddI), stavudine (d4T) and zidovudine (ZDV) were widely used NRTIs.

[1]AIDS Clinical Center, National Center for Global Health and Medicine, Japan, [2]Division of Preventive Medicine, Research Institute, National Center for Global Health and Medicine, Japan and [3]Tokyo Teishin Hospital, Japan
Received for publication September 22, 2010; Accepted for publication December 6, 2010
Correspondence to Dr. Miwako Honda, honda-1@umin.ac.jp